

# Quasi-Monte Carlo for multivariate distributions via generative neural networks

Marius Hofert<sup>1</sup>, Avinash Prasad<sup>2</sup>, Mu Zhu<sup>3</sup>

2022-04-09

## Abstract

Generative moment matching networks (GMMNs) are introduced as quasi-random number generators (QRNGs) for multivariate models with any underlying copula in order to estimate expectations with variance reduction. So far, QRNGs for multivariate distributions required a careful design, exploiting specific properties (such as conditional distributions) of the implied copula or the underlying quasi-Monte Carlo (QMC) point set, and were only tractable for a small number of models. Utilizing GMMNs allows one to construct QRNGs for a much larger variety of multivariate distributions without such restrictions. Once trained with a pseudo-random sample, these neural networks only require a multivariate standard uniform randomized QMC point set as input and are thus fast in estimating expectations of interest under dependence with variance reduction. Numerical examples are considered to demonstrate the approach, including applications inspired by risk management practice. All results are reproducible with the demo HPZ19 as part of the new R package `gnn`; select minimal working examples are provided in the demo `GMMN_QMC` of `gnn`.

## Keywords

maximum mean discrepancy, generative moment matching networks, quasi-random numbers, copulas, sums of dependent random variables, expected shortfall.

## MSC2010

62H99, 65C60, 60E05, 00A72, 65C10.

## 1 Introduction

We consider the problem of estimating an expectation

$$\mathbb{E}(\Psi(\mathbf{X})), \quad (1)$$

---

<sup>1</sup>Department of Statistics and Actuarial Science, University of Waterloo, 200 University Avenue West, Waterloo, ON, N2L 3G1, [marius.hofert@uwaterloo.ca](mailto:marius.hofert@uwaterloo.ca). The author acknowledges support from NSERC (Grant RGPIN-5010-2015).

<sup>2</sup>Department of Statistics and Actuarial Science, University of Waterloo, 200 University Avenue West, Waterloo, ON, N2L 3G1, [a2prasad@uwaterloo.ca](mailto:a2prasad@uwaterloo.ca). The author acknowledges support from NSERC (PGS D Scholarship).

<sup>3</sup>Department of Statistics and Actuarial Science, University of Waterloo, 200 University Avenue West, Waterloo, ON, N2L 3G1, [mu.zhu@uwaterloo.ca](mailto:mu.zhu@uwaterloo.ca). The author acknowledges support from NSERC (RGPIN-2016-03876).

## 1 Introduction

where  $\Psi : \mathbb{R}^d \rightarrow \mathbb{R}$  is a measurable function and  $\mathbf{X} = (X_1, \dots, X_d)$  is a  $d$ -dimensional random vector with distribution function  $F_{\mathbf{X}}$ . In this paper, we focus on  $F_{\mathbf{X}}$  being continuous and decomposable into margins  $F_{X_1}, \dots, F_{X_d}$  and copula  $C$  by Sklar's theorem; see Nelsen (2006) or Joe (2014) for an introduction to copulas. Since, in distribution,  $\mathbf{X} = F_{\mathbf{X}}^{-1}(\mathbf{U})$  for  $\mathbf{U} \sim C$  and  $F_{\mathbf{X}}^{-1}(\mathbf{u}) = (F_{X_1}^{-1}(u_1), \dots, F_{X_d}^{-1}(u_d))$ , the quantity (1) is equivalent to

$$\mathbb{E}(\Psi(F_{\mathbf{X}}^{-1}(\mathbf{U}))). \quad (2)$$

The *(crude) Monte Carlo estimator* approximates this expectation by

$$\frac{1}{n} \sum_{i=1}^n \Psi(F_{\mathbf{X}}^{-1}(\mathbf{U}_i)), \quad (3)$$

where  $\mathbf{U}_1, \dots, \mathbf{U}_n \stackrel{\text{ind.}}{\sim} C$ .

If  $C$  is the independence copula  $\Pi(\mathbf{u}) = \prod_{j=1}^d u_j$ , one can achieve variance reduction when estimating (2) with (3) by utilizing a randomized quasi-Monte Carlo (RQMC) approach – one simply replaces  $\mathbf{U}_1, \dots, \mathbf{U}_n \stackrel{\text{ind.}}{\sim} \Pi$  by an RQMC point set such as a randomized Sobol' sequence or a generalized Halton sequence; see, for example, Lemieux (2009, Chapters 5).

Recently, Cambou et al. (2017) introduced  $p$ -to- $d$  transformations (for  $p \geq d$ ; typically  $p = d$  or  $p = d + 1$ ) of RQMC point sets to samples which mimic samples from  $C$  but preserve low discrepancy in the sense of being locally more homogeneous (producing less “gaps” or “clusters”); see Cambou et al. (2017, Section 4.2) for the technical details including the notion of (star-)copula-discrepancy. When applied to an RQMC point set, we will informally refer to such transformations as *quasi-random number generators (QRNGs)* for  $C$  or  $F_{\mathbf{X}}$ . The major problem is that for  $C \neq \Pi$ , the transformations underlying QRNGs are only available in numerically tractable form for a few specific models  $C$ ; see Cambou et al. (2017). What is available for all copulas  $C$  of practical interest, however, is a *pseudo-random number generator (PRNG)* for  $C$ , that is, a stochastic representation of  $\mathbf{U} \sim C$  which can be used for efficient sampling (fast and numerically reliable).

The main contribution of this paper is to introduce a new approach for constructing QRNGs for  $F_{\mathbf{X}}$  with any underlying copula  $C$ , using pre-trained generative neural networks, and to show that it can act as a variance reduction method. Our approach utilizes generative moment matching networks (GMMNs) to conceptually construct an approximation  $\mathbf{Y}$  to  $\mathbf{X}$  and, as an approximation to (1), it uses

$$\frac{1}{n} \sum_{i=1}^n \Psi(\mathbf{Y}_i) \quad (4)$$

for

$$\mathbf{Y}_i = f_{\hat{\theta}} \circ F_{\mathbf{Z}}^{-1}(\tilde{\mathbf{v}}_i), \quad i = 1, \dots, n, \quad (5)$$

where  $\{\tilde{\mathbf{v}}_1, \dots, \tilde{\mathbf{v}}_n\}$  is a  $p$ -dimensional RQMC point set;  $F_{\mathbf{Z}}^{-1}(\mathbf{u}) = (F_{Z_1}^{-1}(u_1), \dots, F_{Z_p}^{-1}(u_p))$  is a mapping from the RQMC point set to the prior distribution of the GMMN  $f_{\hat{\theta}}$  with parameters  $\hat{\theta}$ , trained based on pseudo-random samples from  $F_{\mathbf{X}}$  or, equivalently, pseudo-observations from the corresponding [C Hofert et al. \(2018, Section 4.1.2\)](#). Later we explain in more detail (see Section 2.3) that well-trained GMMNs produce a smooth mapping  $f_{\hat{\theta}}$ ; if  $\Psi$  is also a sufficiently smooth function, this guarantees that the estimation error of (1) by (4) is small.

In Section 2, we provide a brief introduction to GMMNs and explain the above approximation in more detail. In Section 3, we address the training of GMMNs and assess the accuracy of GMMN-generated samples for various copula models. In Section 4, we numerically investigate the variance-reduction property of different QRNG-based estimators in a number of applications. In Section 5, we discuss some key open questions for future work. Some theoretical results are given in the appendix. Note that all figures presented in this paper (and more) are reproducible via the demo `HPZ19` provided in R package `gnn`; see also the demo `GMMN_QMC` for select minimal working examples.

## 2 Quasi-random GMMN samples

### 2.1 Generative moment matching networks

We now introduce the notation for the deep neural networks we use. The *multi-layer perceptron (MLP)* is the quintessential deep neural network, which we simply refer to as *neural network (NN)* in what follows. Let  $L$  be the number of (hidden) layers in the NN and, for each  $l = 0, \dots, L + 1$ , let  $d_l$  be the dimension of layer  $l$ , that is, the number of neurons in layer  $l$ . In this notation, layer  $l = 0$  refers to the *input layer* which consists of the *input*  $\mathbf{z} \in \mathbb{R}^p$  for  $d_0 = p$ , and layer  $l = L + 1$  refers to the *output layer* which consists of the *output*  $\mathbf{y} \in \mathbb{R}^d$  for  $d_{L+1} = d$ . Layers  $l = 1, \dots, L + 1$  can be described in terms of the output  $\mathbf{a}_{l-1} \in \mathbb{R}^{d_{l-1}}$  of layer  $l - 1$  via

$$\begin{aligned}\mathbf{a}_0 &= \mathbf{z} \in \mathbb{R}^{d_0}, \\ \mathbf{a}_l &= f_l(\mathbf{a}_{l-1}) = \phi_l(W_l \mathbf{a}_{l-1} + \mathbf{b}_l) \in \mathbb{R}^{d_l}, \quad l = 1, \dots, L + 1, \\ \mathbf{y} &= \mathbf{a}_{L+1} \in \mathbb{R}^{d_{L+1}},\end{aligned}$$

with *weight matrices*  $W_l \in \mathbb{R}^{d_l \times d_{l-1}}$ , *bias vectors*  $\mathbf{b}_l \in \mathbb{R}^{d_l}$  and *activation functions*  $\phi_l$ ; note that for vector inputs the activation function  $\phi_l$  is understood to be applied componentwise.

The NN  $f_{\theta} : \mathbb{R}^p \leftarrow \mathbb{R}^d$  can then be written as the composition

$$f_{\theta} = f_{L+1} \circ f_L \circ \dots \circ f_2 \circ f_1,$$

with its (flattened) parameter vector given by  $\theta = (W_1, \dots, W_{L+1}, \mathbf{b}_1, \dots, \mathbf{b}_{L+1})$ . To fit  $\theta$ , we use the backpropagation algorithm (a stochastic gradient descent) based on a *cost function*  $E$  between the *target output*  $\mathbf{x} = \mathbf{x}(\mathbf{z}) \in \mathbb{R}^{d_{L+1}}$  and the *actual output*  $\mathbf{y} \in \mathbb{R}^{d_{L+1}}$  predicted by the NN.

The expressive power of NNs is primarily characterized by the *universal approximation theorem*; see Goodfellow et al. (2016, Chapter 6). In particular, given suitable activation functions, a single-layer NN with a finite number of neurons can approximate any continuous function on a compact subset of the multidimensional Euclidean space; see Nielsen (2015, Chapter 4) for a visual and interactive account of the validity of the universal approximation theorem. Cybenko (1989) first proposed such universal approximation results for the sigmoid activation function,  $\phi_l(x) = 1/(1 + e^{-x})$  and Hornik (1991, Theorem 1) then generalized the results to include arbitrary bounded and non-constant activation functions. In recent years, the *rectified linear unit (ReLU)*  $\phi_l(x) = \max\{0, x\}$  has become the most popular activation function for efficiently training NNs. This unbounded activation function does not satisfy the assumptions of the universal approximation theorem in Hornik (1991). However, there have since been numerous theoretical investigations into the expressive power of deep NNs with ReLU activation functions; see, for example, Pascanu et al. (2013), Montufar et al. (2014) or Arora, Basu, et al. (2016). In particular, for certain conditions on the number of layers and neurons in the NN, Arora, Basu, et al. (2016) provide a similar universal approximation theorem for NNs with ReLU activation functions.

Li et al. (2015) and Dziugaite et al. (2015) simultaneously introduced a type of generative neural network known as *generative moment matching networks (GMMNs)* or Maximum Mean Discrepancy (MMD) nets. GMMNs are NNs  $f_{\theta}$  of the above form which utilize a (kernel) maximum mean discrepancy statistic as the cost function (see later). Conceptually, they can be thought of as parametric maps of a given sample  $\mathbf{Z} = (Z_1, \dots, Z_p)$  from a *prior distribution*  $F_{\mathbf{Z}}$  to a sample  $\mathbf{X} = (X_1, \dots, X_d)$  from the *target distribution*  $F_{\mathbf{X}}$ . As is standard in the literature, we assume independence among the components of  $\mathbf{Z} = (Z_1, \dots, Z_p)$ . Typical choices for the distribution of the  $Z_j$ 's are  $U(0, 1)$  or  $N(0, 1)$ . The objective is then to generate samples from the target distribution via the GMMN  $f_{\theta} : \mathbb{R}^p \rightarrow \mathbb{R}^d$  which represents the deterministic mapping from a sample from the prior distribution to a sample from the target distribution. The MMD nets introduced in Dziugaite et al. (2015) are almost identical to GMMNs but with a slight difference in the training procedure. Additionally, Dziugaite et al. (2015) provided a theoretical framework for analyzing (in general) optimization algorithms with (kernel) MMD cost functions.

## 2.2 Cost function and training of GMMNs

To learn  $f_{\theta}$  (or, statistically speaking, to estimate the parameters  $\theta$ ) we assume to have  $n_{\text{trn}}$  training data points  $\mathbf{X}_1, \dots, \mathbf{X}_{n_{\text{trn}}}$  from  $\mathbf{X}$ . Based on an input sample  $\mathbf{Z}_1, \dots, \mathbf{Z}_{n_{\text{trn}}}$  from the prior distribution, the GMMN generates the output sample  $\mathbf{Y}_1, \dots, \mathbf{Y}_{n_{\text{trn}}}$ , where  $\mathbf{Y}_i = f_{\theta}(\mathbf{Z}_i)$ ,  $i = 1, \dots, n_{\text{trn}}$ . We are thus interested in whether the two samples  $X = (\mathbf{X}_1^\top, \dots, \mathbf{X}_{n_{\text{trn}}}^\top)^\top \in \mathbb{R}^{n_{\text{trn}} \times d}$  and  $Y = (\mathbf{Y}_1^\top, \dots, \mathbf{Y}_{n_{\text{trn}}}^\top)^\top \in \mathbb{R}^{n_{\text{trn}} \times d}$  come from the same distribution.

To this end, GMMNs utilize as cost function  $E$  the *maximum mean discrepancy (MMD)* statistic from the kernel two-sample test introduced by Gretton et al. (2007), whose sample

version is given by

$$\text{MMD}(X, Y) = \sqrt{\frac{1}{n_{\text{trn}}^2} \sum_{i_1=1}^{n_{\text{trn}}} \sum_{i_2=1}^{n_{\text{trn}}} (K(\mathbf{X}_{i_1}, \mathbf{X}_{i_2}) - 2K(\mathbf{X}_{i_1}, \mathbf{Y}_{i_2}) + K(\mathbf{Y}_{i_1}, \mathbf{Y}_{i_2})),} \quad (6)$$

where  $K(\cdot, \cdot) : \mathbb{R}^d \times \mathbb{R}^d \rightarrow \mathbb{R}$  denotes a kernel (similarity) function. If  $K(\cdot, \cdot)$  is a so-called universal kernel function (e.g., Gaussian or Laplace), then it can be shown Gretton et al. (2007) and Gretton et al. (2012) that the MMD converges in probability to 0 for  $n_{\text{trn}} \rightarrow \infty$  if and only if  $\mathbf{Y} = \mathbf{X}$  in distribution. Minimizing the MMD with a universal kernel function can thus be interpreted as matching all the moments of the distributions of  $\mathbf{X}$  and  $\mathbf{Y}$ , hence making MMD an intuitive choice as cost function for training  $f_{\theta}$  to learn a random number generator from a multivariate distribution; our choice of kernel  $K$  is addressed in Section 3.1.

As suggested by Li et al. (2015), we adopt a mini-batch optimization procedure. This is necessary because the MMD-criterion (6) would otherwise require the evaluation of all  $\binom{n_{\text{trn}}}{2}$  pairs of observations, which is memory-prohibitive for even moderately large  $n_{\text{trn}}$ . Rather than directly optimizing the MMD for the entire training dataset, we partition it into *batches* of size  $n_{\text{bat}}$  and use the batches sequentially to update the parameters  $\theta$  of the GMMN using the Adam optimizer of Kingma and Ba (2014). Instead of following the gradient at each iterative step, the Adam optimizer essentially uses a “memory-sticking gradient” – a weighted combination of the current gradient and past gradients from earlier iterations. After all the training data are exhausted, i.e., roughly after  $(n_{\text{trn}}/n_{\text{bat}})$ -many batches or gradient steps, one *epoch* of the training of the GMMN is completed. The overall training procedure is considered completed after  $n_{\text{epo}}$  epochs. The training of the GMMN can thus be summarized as follows:

### Algorithm 2.1 (Training GMMNs)

- 1) Fix the number  $n_{\text{epo}}$  of epochs and the batch size  $1 \leq n_{\text{bat}} \leq n_{\text{trn}}$  per epoch, where  $n_{\text{bat}}$  is assumed to divide  $n_{\text{trn}}$ . Initialize the epoch counter  $k = 0$  and the GMMN’s parameter vector  $\theta = \theta^{(0)}$ ; we follow Glorot and Bengio (2010) and initialize the components of  $\theta^{(0)}$  as  $W_l \sim U(-\sqrt{6/(d_l + d_{l-1})}, \sqrt{6/(d_l + d_{l-1})})^{d_l \times d_{l-1}}$  and  $\mathbf{b}_l = \mathbf{0}$  for  $l = 1, \dots, L + 1$ .
- 2) For epoch  $k = 1, \dots, n_{\text{epo}}$ , do:
  - 2.1) Randomly partition the prior distribution sample  $\mathbf{Z}_1, \dots, \mathbf{Z}_{n_{\text{trn}}}$  and training sample  $\mathbf{X}_1, \dots, \mathbf{X}_{n_{\text{trn}}}$  into corresponding  $n_{\text{trn}}/n_{\text{bat}}$  non-overlapping batches  $\mathbf{Z}_1^{(b)}, \dots, \mathbf{Z}_{n_{\text{bat}}}^{(b)}$  and  $\mathbf{X}_1^{(b)}, \dots, \mathbf{X}_{n_{\text{bat}}}^{(b)}$ ,  $b = 1, \dots, n_{\text{trn}}/n_{\text{bat}}$ , of size  $n_{\text{bat}}$  each.
  - 2.2) For batch  $b = 1, \dots, n_{\text{trn}}/n_{\text{bat}}$ , do:
    - 2.2.1) Compute the GMMN output  $\mathbf{Y}_i^{(b)} = f_{\theta^{(k-1)}}(\mathbf{Z}_i^{(b)})$ ,  $i = 1, \dots, n_{\text{bat}}$ .
    - 2.2.2) Compute the gradient  $\frac{\partial}{\partial \theta} \text{MMD}(X^{(b)}, Y^{(b)})$  from the samples  $X^{(b)} = (\mathbf{X}_1^{(b)\top}, \dots, \mathbf{X}_{n_{\text{bat}}}^{(b)\top})^\top$  and  $Y^{(b)} = (\mathbf{Y}_1^{(b)\top}, \dots, \mathbf{Y}_{n_{\text{bat}}}^{(b)\top})^\top$ , for example, via automatic differentiation.

2.2.3) Take a gradient step to update  $\boldsymbol{\theta}^{(k-1)}$  to  $\boldsymbol{\theta}^{(k)}$  according to Adam; see Kingma and Ba (2014, Algorithm 1).

3) Return  $\hat{\boldsymbol{\theta}} = \boldsymbol{\theta}^{(n_{\text{epoch}})}$ ; the fitted GMMN is then  $f_{\hat{\boldsymbol{\theta}}}$ .

### 2.3 GMMN PRNGs and GMMN QRNGs

The following algorithm describes a PRNG from  $\mathbf{Y}$  via the trained GMMN  $f_{\hat{\boldsymbol{\theta}}}$  based on a PRNG for the random vector  $\mathbf{Z}$  from the prior distribution  $F_{\mathbf{Z}}$ .

#### Algorithm 2.2 (GMMN PRNG)

- 1) Fix the number  $n_{\text{gen}}$  of samples to generate from  $\mathbf{Y}$ .
- 2) Draw  $\mathbf{Z}_i \stackrel{\text{ind.}}{\sim} F_{\mathbf{Z}}$ ,  $i = 1, \dots, n_{\text{gen}}$ , for example, via  $\mathbf{Z}_i = F_{\mathbf{Z}}^{-1}(\mathbf{U}'_i)$ ,  $i = 1, \dots, n_{\text{gen}}$ , where  $\mathbf{U}'_1, \dots, \mathbf{U}'_{n_{\text{gen}}} \stackrel{\text{ind.}}{\sim} \text{U}(0, 1)^p$ .
- 3) Return  $\mathbf{Y}_i = f_{\hat{\boldsymbol{\theta}}}(\mathbf{Z}_i)$ ,  $i = 1, \dots, n_{\text{gen}}$ .

To construct a QRNG for  $F_{\mathbf{X}}$  with underlying copula  $C$ , we replace  $\mathbf{U}'_1, \dots, \mathbf{U}'_{n_{\text{gen}}} \stackrel{\text{ind.}}{\sim} \text{U}(0, 1)^p$  in Algorithm 2.2 by an RQMC point set to obtain the following algorithm; the randomization is done to obtain unbiased QMC estimators and estimates of their variances.

#### Algorithm 2.3 (GMMN QRNG)

- 1) Fix the number  $n_{\text{gen}}$  of samples to generate from  $\mathbf{Y}$ .
- 2) Compute an RQMC point set  $\tilde{P}_{n_{\text{gen}}} = \{\tilde{\mathbf{v}}_1, \dots, \tilde{\mathbf{v}}_{n_{\text{gen}}}\}$  (for example, a randomized Sobol' or a generalized Halton sequence) and  $\mathbf{Z}_i = F_{\mathbf{Z}}^{-1}(\tilde{\mathbf{v}}_i)$ ,  $i = 1, \dots, n_{\text{gen}}$ .
- 3) Return  $\mathbf{Y}_i = f_{\hat{\boldsymbol{\theta}}}(\mathbf{Z}_i)$ ,  $i = 1, \dots, n_{\text{gen}}$ .

Note that  $\tilde{P}_{n_{\text{gen}}}$  mimics  $\text{U}(0, 1)^p$ , and not  $C$ . As mentioned in the introduction, Cambou et al. (2017) presented transformations to convert  $\tilde{P}_{n_{\text{gen}}}$  to samples which mimic samples from  $C$  but locally provide a more homogeneous coverage. Unfortunately, these transformations are only available mathematically for a few specific cases of  $C$  and their numerical evaluation in a fast and numerically robust way is even more challenging. Both speed and numerical robustness are important, as otherwise RQMC estimates typically lose their advantages over crude Monte Carlo estimates.

To avoid these problems, we suggest to utilize the GMMN  $f_{\hat{\boldsymbol{\theta}}}$  trained as in Algorithm 2.1. Besides a fast and numerically straightforward evaluation, this allows us to generate quasi-random samples from  $F_{\mathbf{X}}$  with any underlying copula  $C$ , by training a GMMN on pseudo-random samples generated from  $F_{\mathbf{X}}$ . Alternatively, quasi-random samples which follow the same empirical distribution as any given data set can be obtained by directly training a GMMN on the data set itself. An additional advantage is that GMMNs provide a sufficiently smooth map from the RQMC point set to the target distribution which helps preserve (in a sense) the low-discrepancy of the point set upon transformation and hence

## 2 Quasi-random GMMN samples

guarantees the improved performance of RQMC estimators compared to the MC estimator (see later).

With the mapping  $F_{\mathbf{Z}}^{-1}(\mathbf{u}) = (F_{Z_1}^{-1}(u_1), \dots, F_{Z_p}^{-1}(u_p))$  to the prior distribution and the trained GMMN  $f_{\hat{\theta}}$  at hand, define a transform

$$q(\mathbf{u}) = f_{\hat{\theta}} \circ F_{\mathbf{Z}}^{-1}(\mathbf{u}), \quad \mathbf{u} \in (0, 1)^p.$$

Based on the RQMC point set  $\tilde{P}_{n_{\text{gen}}} = \{\tilde{\mathbf{v}}_1, \dots, \tilde{\mathbf{v}}_{n_{\text{gen}}}\}$  of size  $n_{\text{gen}}$  we can then define the *GMMN QRNG* by

$$\mathbf{Y}_i = q(\tilde{\mathbf{v}}_i), \quad i = 1, \dots, n_{\text{gen}},$$

(compare with (5)) and the *GMMN RQMC estimator* of (1) by

$$\mu_{n_{\text{gen}}} = \frac{1}{n_{\text{gen}}} \sum_{i=1}^{n_{\text{gen}}} \Psi(\mathbf{Y}_i) = \frac{1}{n_{\text{gen}}} \sum_{i=1}^{n_{\text{gen}}} \Psi(q(\tilde{\mathbf{v}}_i)) = \frac{1}{n_{\text{gen}}} \sum_{i=1}^{n_{\text{gen}}} \Psi(f_{\hat{\theta}}(F_{\mathbf{Z}}^{-1}(\tilde{\mathbf{v}}_i))). \quad (7)$$

We thus have the approximations

$$\mathbb{E}(\Psi(\mathbf{X})) \approx \mathbb{E}(\Psi(\mathbf{Y})) \approx \mu_{n_{\text{gen}}}. \quad (8)$$

The error in the first approximation is small if the GMMN is trained well and the error in the second approximation is small if the unbiased estimator  $\mu_{n_{\text{gen}}}$  has a small variance. The primary *bottleneck* in this setup is the error in the first approximation which is determined by the size  $n_{\text{trn}}$  of the training data set and, in particular, by the batch size  $n_{\text{bat}}$  which is the major factor determining training efficiency of the GMMN we found in our numerical studies conducted in Sections 3 and 4. Given a sufficiently large  $n_{\text{bat}}$  and, by extension,  $n_{\text{trn}}$ , the GMMN is trained well, which renders the first approximation error in (8) negligible. However, in practice the batch size  $n_{\text{bat}}$  is constrained by the quadratically increasing memory demands to compute the MMD loss function of the GMMN. For a theoretical result regarding this approximation error, see Dziugaite et al. (2015) where a bound on the error between optimizing a sample version and a population version of  $\text{MMD}(X, Y)$  was investigated. Finally, let us note that the task of GMMN training and generation are separate steps which ensures that, once trained, generating quasi-random GMMN samples is fast.

The error in the second approximation in (8) is small if the composite function  $\Psi \circ q$  is sufficiently smooth. The transform  $q$  is sufficiently smooth for GMMNs  $f_{\hat{\theta}}$  constructed using standard activation functions and commonly used prior distributions; see the discussion following Corollary A.4. Given a sufficiently smooth  $\Psi$ , we can establish a rate of convergence for the variance (and for the approximation error) of GMMN RQMC estimators constructed using the scrambling method for randomization; see Appendix A.4.1. With a stronger assumption on the behavior of the composite function  $\Psi \circ q$ , we can show that the Koksma–Hlawka bound on the error between the (non-randomized) GMMN QMC estimator

$\frac{1}{n_{\text{gen}}} \sum_{i=1}^{n_{\text{gen}}} \Psi(q(\mathbf{v}_i))$  and  $\mathbb{E}(\Psi(\mathbf{Y}))$  is satisfied which in turn implies a convergence rate for the (non-randomized) GMMN QMC estimator; see Appendix A.2. If the Koksma–Hlawka bound holds, we can also establish a convergence rate for the variance of GMMN RQMC estimators constructed using the digital shift method as randomization technique; see Appendix A.4.2.

### 3 GMMN PRNGs and QRNGs for copula models

Since we want to investigate the quality of  $\mathbf{Y}_1, \dots, \mathbf{Y}_{n_{\text{gen}}}$ , we train GMMNs on training data  $\mathbf{U}_1, \dots, \mathbf{U}_{n_{\text{trn}}} \sim C$  generated from a PRNG from the respective copula  $C$ , using, for example, the function `rCopula()` of the R package `copula`. We start by addressing key implementation details and hyperparameters of Algorithm 2.1 that we used in all examples thereafter. By utilizing this algorithm to train  $f_{\theta}$  for a wide variety of copula families, we then investigate the quality of  $\mathbf{Y}_1, \dots, \mathbf{Y}_{n_{\text{gen}}}$ , once generated by Algorithm 2.2 and once by Algorithm 2.3. If the conceptual random vector  $\mathbf{Y}$  follows a target copula, so has  $U(0, 1)$  margins, we equip Algorithms 2.2 and 2.3 with a minor post-processing step by returning the pseudo-observations based on  $\mathbf{Y}_1, \dots, \mathbf{Y}_{n_{\text{gen}}}$ , see Hofert et al. (2018, Section 4.1.2), to remove any residual marginal non-uniformity from the GMMN samples. To generate the RQMC point set in Algorithm 2.3, we use scrambled nets Owen (1995); see also Appendix A.3. Specifically, we use the implementation `sobol()`, `randomize = "Owen"` from the R package `qrng`.

#### 3.1 GMMN architecture, choice of kernel and training setup

We find a one-layer architecture ( $L = 1$ ) to be sufficient for the examples considered which is in line with the universal approximation theorem. After experimentation, we fix  $d_1 = 300$ ,  $\phi_1$  to be ReLU (it offers computational efficiency via non-expensive and non-vanishing gradients) and  $\phi_2$  to be sigmoid (to obtain outputs in  $[0, 1]^d$ ).

We follow Li et al. (2015) and use a mixture of Gaussian kernels with different bandwidth parameters as kernel function for the MMD statistic in (6), that is, we utilize the kernel

$$K(\mathbf{x}, \mathbf{y}) = \sum_{i=1}^{n_{\text{kern}}} K(\mathbf{x}, \mathbf{y}; \sigma_i), \quad (9)$$

where  $n_{\text{kern}}$  denotes the number of mixture components and  $K(\mathbf{x}, \mathbf{y}; \sigma) = \exp(-\|\mathbf{x} - \mathbf{y}\|_2^2 / (2\sigma^2))$  is the Gaussian Kernel with bandwidth parameter  $\sigma > 0$ . After experimentation, we fix  $n_{\text{kern}} = 6$  and choose  $(\sigma_1, \dots, \sigma_6) = (0.001, 0.01, 0.15, 0.25, 0.50, 0.75)$ ; note that we work with copula samples which are in  $[0, 1]^d$ .

Unless otherwise specified, we use the following setup across all examples. We use  $n_{\text{trn}} = 60\,000$  training data points and find this to be sufficiently large to obtain reliable  $f_{\hat{\theta}}$ . As dimension of the prior distribution  $F_Z$ , we choose  $p = d$ , that is, the GMMN  $f_{\theta}$  is set to be a  $d$ -to- $d$  transformation. For  $F_Z$ , we choose  $\mathbf{Z} \sim N(\mathbf{0}, I_d)$ , where  $I_d$  denotes the identity

matrix in  $\mathbb{R}^{d \times d}$ , so  $\mathbf{Z}$  consists of independent standard normal random variables; this choice worked better than  $\text{U}(0, 1)^d$  in practice despite the fact that  $\text{N}(\mathbf{0}, I_d)$  does not satisfy the assumptions of Proposition A.1. We choose a batch size of  $n_{\text{bat}} = 5000$  in Algorithm 2.1; this decision is motivated from a practical trade-off that a small  $n_{\text{bat}}$  will lead to poor estimates of the population MMD cost function but a large  $n_{\text{bat}}$  will incur quadratically growing memory requirements due to (6). As the number of epochs we choose  $n_{\text{epo}} = 300$  which is generally sufficient in our experiments to obtain accurate results. The tuning parameters of the Adam optimizer is set to the default values reported in Kingma and Ba (2014).

All our experiments and examples are implemented in R and can be reproduced using the demo HPZ19 provided as part of the newly developed R package `gnn`. In our implementation, we make use of the R packages `keras` and `tensorflow`, which serve as R interfaces to the corresponding namesake Python libraries. Furthermore, all GMMN training is carried out on four NVIDIA Tesla P100 GPUs with 16GB RAM each.

### 3.2 Visual assessments of GMMN samples

In this section we primarily focus on the bivariate case but include an example involving a trivariate copula; for higher-dimensional copulas, see Sections 3.3 and 4. For all one-parameter copulas considered, the single parameter will be chosen such that Kendall's tau, denoted by  $\tau$ , is equal to 0.25 (weak dependence), 0.50 (moderate dependence) or 0.75 (strong dependence); clearly, this only applies to copula families where there is a one-to-one mapping between the copula parameter and  $\tau$ .

#### 3.2.1 $t$ , Archimedean copulas and their associated mixtures

First, we consider Student  $t$  copulas, Archimedean copulas, and their mixtures.

Student  $t$  copulas are prominent members of the elliptical class of copulas and are given by  $C(\mathbf{u}) = t_{\nu, P}(t_{\nu}^{-1}(u_1), \dots, t_{\nu}^{-1}(u_d))$ ,  $\mathbf{u} \in [0, 1]^d$ , where  $t_{\nu, P}$  denotes the distribution function of the  $d$ -dimensional  $t$  distribution with  $\nu$  degrees of freedom, location vector  $\mathbf{0}$  and scale matrix  $P$  (a correlation matrix), and  $t_{\nu}^{-1}$  denotes the quantile function of the univariate  $t$  distribution with  $\nu$  degrees of freedom. For all  $t$  copulas considered in this work, we fix  $\nu = 4$ . Student  $t$  copulas have explicit inverse Rosenblatt transforms, which can be used to obtain QRNGs; see Cambou et al. (2017). Note that sampling via the inverse Rosenblatt transform is also referred to as the conditional distribution method (CDM).

Archimedean copulas are copulas of the form

$$C(\mathbf{u}) = \psi(\psi^{-1}(u_1), \dots, \psi^{-1}(u_d)), \quad \mathbf{u} \in [0, 1]^d,$$

for an Archimedean generator  $\psi$  which is a continuous, decreasing function  $\psi : [0, \infty] \rightarrow [0, 1]$  which satisfies  $\psi(0) = 1$ ,  $\psi(\infty) = \lim_{t \rightarrow \infty} \psi(t) = 0$  and which is strictly decreasing on  $[0, \inf t : \psi(t) = 0]$ . Examples of Archimedean generators include  $\psi_C(t) = (1 + t)^{-1/\theta}$  (for  $\theta > 0$ ) and  $\psi_G(t) = \exp(-t^{1/\theta})$  (for  $\theta \geq 1$ ), generating Clayton and Gumbel copulas,

respectively. In contrast to Gumbel copulas, for Clayton copulas we can obtain QRNGs via an explicit inverse Rosenblatt transform.

We additionally consider equally-weighted two-component mixture copulas, in which one component is a 90-degree-rotated  $t_4$  copula with  $\tau = 0.5$  and the other component is either a Clayton copula ( $\tau = 0.50$ ) or a Gumbel copula ( $\tau = 0.50$ ). The two mixture copula models are referred to as Clayton- $t$ (90) and Gumbel- $t$ (90) copulas, respectively.

The top rows of Figures 1–3 display contour plots of true  $t$ , Clayton and Gumbel copulas respectively, with  $\tau = 0.25$  (left), 0.50 (middle) and 0.75 (right) along with contours of empirical copulas based on GMMN PRNG and GMMN QRNG samples corresponding to each true copula  $C$ . The top row of Figure 4 displays similar plots for Clayton- $t$ (90) (left) and Gumbel- $t$ (90) (right) copulas. In each plot, across all figures described above, we observe that the contour of the empirical copula based on GMMN PRNG samples is visually fairly similar to the contour of  $C$ , thus indicating that the 11 GMMNs have been trained sufficiently well. We also see that the contours of the empirical copulas based on GMMN QRNG samples better approximate the contours of  $C$  than the contours of the empirical copulas based on GMMN PRNG samples. This observation indicates that, at least visually, the 11 GMMN transforms (corresponding to each  $C$ ) have (in a sense) preserved the low discrepancy of the input RQMC point sets.

The bottom rows of Figures 1–4 display Rosenblatt transformed GMMN QRNG samples, corresponding to each of the 11 true copulas  $C$  under consideration. The Rosenblatt transform  $\mathcal{R}$ , see Rosenblatt (1952), for a bivariate copula  $C$  maps  $(U_1, U_2) \sim C$  to  $(R_1, R_2) = (U_1, C_{2|1}(U_2 | U_1))$ , where  $C_{2|1}(u_2 | u_1)$  denotes the conditional distribution function of  $U_2$  given  $U_1 = u_1$  under  $C$ . We exploit the fact that  $(R_1, R_2) \sim U(0, 1)^2$  if and only if  $(U_1, U_2) \sim C$ . Moreover, applying  $\mathcal{R}$  to the post-processed GMMN QRNG samples should yield a more homogeneous coverage of  $[0, 1]^2$ . From each of the scatter plots in Figures 1–4, we observe no significant departure from  $U(0, 1)^2$ , thus indicating that the GMMNs have learned sufficient approximations to the corresponding true copulas  $C$ . Furthermore, the lack of gaps or cluster in the scatter plots provides some visual confirmation of the low discrepancy of the Rosenblatt-transformed GMMN QRNG samples.

### 3.2.2 Nested Archimedean, Marshall–Olkin and mixture copulas

Next, we consider more complex copulas such as nested Archimedean copulas and Marshall–Olkin copulas. We also re-consider the two mixture copulas introduced in the previous section along with an additional mixture copula. To better showcase the complexity of these dependence structures, we use scatter plots instead of contour plots to display copula and GMMN-generated samples. We omit the plots containing the Rosenblatt transformed samples since they are harder to obtain for the copulas we investigate in this section.

Nested Archimedean copulas (NACs) are Archimedean copulas with arguments possibly replaced by other NACs; see McNeil (2008) or Hofert (2012). In particular, this class of copulas allows to construct asymmetric extensions of Archimedean copulas. Important to note here is that NACs are copulas for which there is no known (tractable) QRNG. To

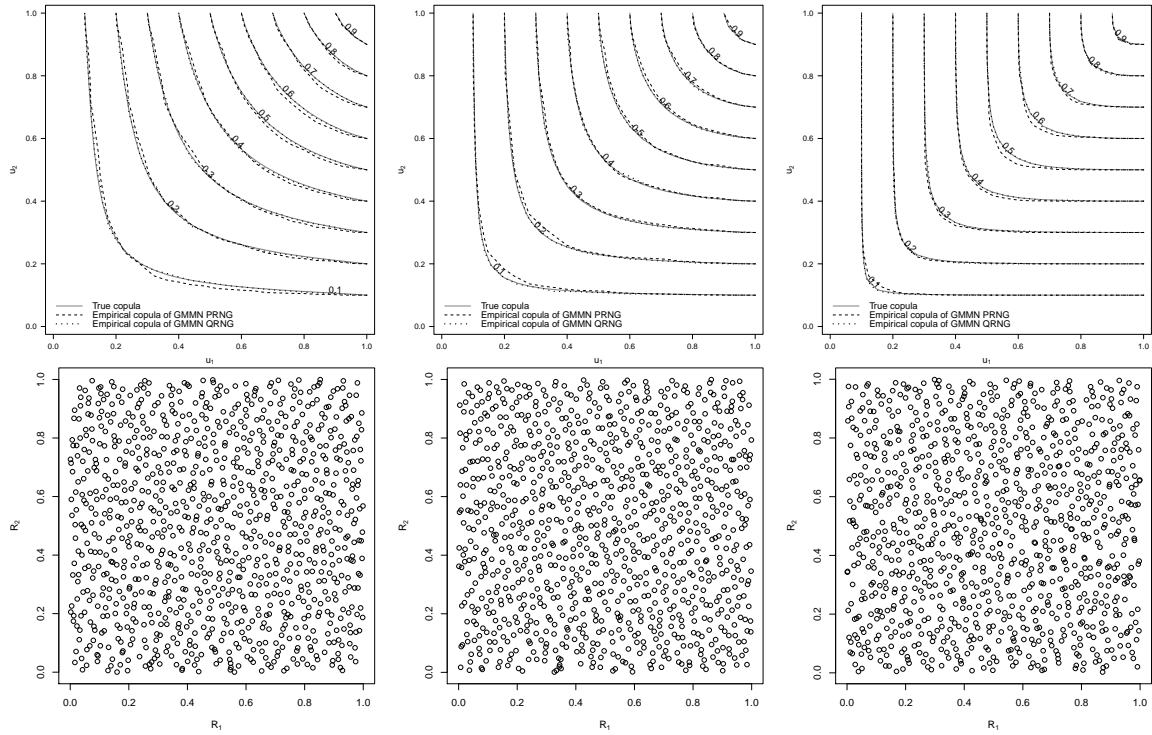


**Figure 1** Top row contains contour plots of true  $t_4$  copulas with  $\tau = 0.25$  (left),  $0.50$  (middle) and  $0.75$  (right) along with the corresponding contour plots of empirical copulas based on GMMN PRNG and GMMN QRNG samples of size  $n_{\text{gen}} = 1000$ . Bottom row contains Rosenblatt-transformed GMMN QRNG samples corresponding to the same  $t_4$  copulas.

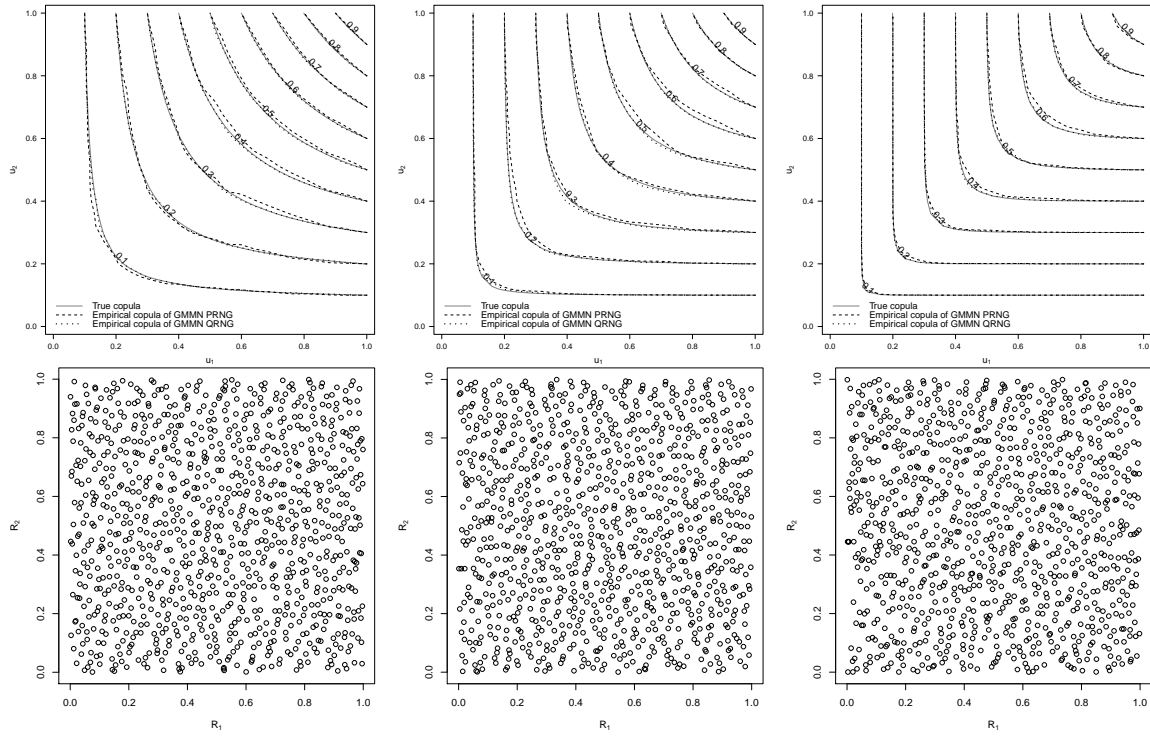


**Figure 2** Top row contains contour plots of true Clayton copulas with  $\tau = 0.25$  (left),  $0.50$  (middle) and  $0.75$  (right) along with the corresponding contour plots of empirical copulas based on GMMN PRNG and GMMN QRNG samples of size  $n_{\text{gen}} = 1000$ . Bottom row contains Rosenblatt-transformed GMMN QRNG samples corresponding to the same Clayton copulas.

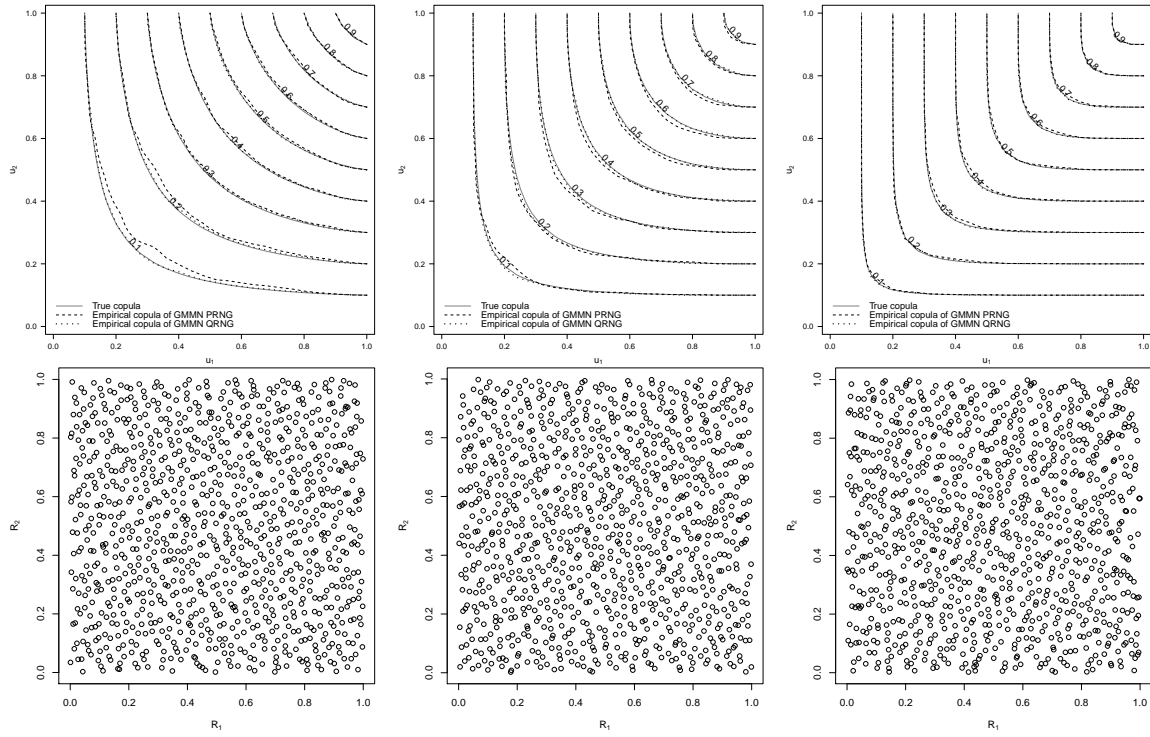


**Figure 3** Top row contains contour plots of true Gumbel copulas with  $\tau = 0.25$  (left),  $0.50$  (middle) and  $0.75$  (right) along with the corresponding contour plots of empirical copulas based on GMMN PRNG and GMMN QRNG samples of size  $n_{\text{gen}} = 1000$ . Bottom row contains Rosenblatt-transformed GMMN QRNG samples corresponding to the same Gumbel copulas.

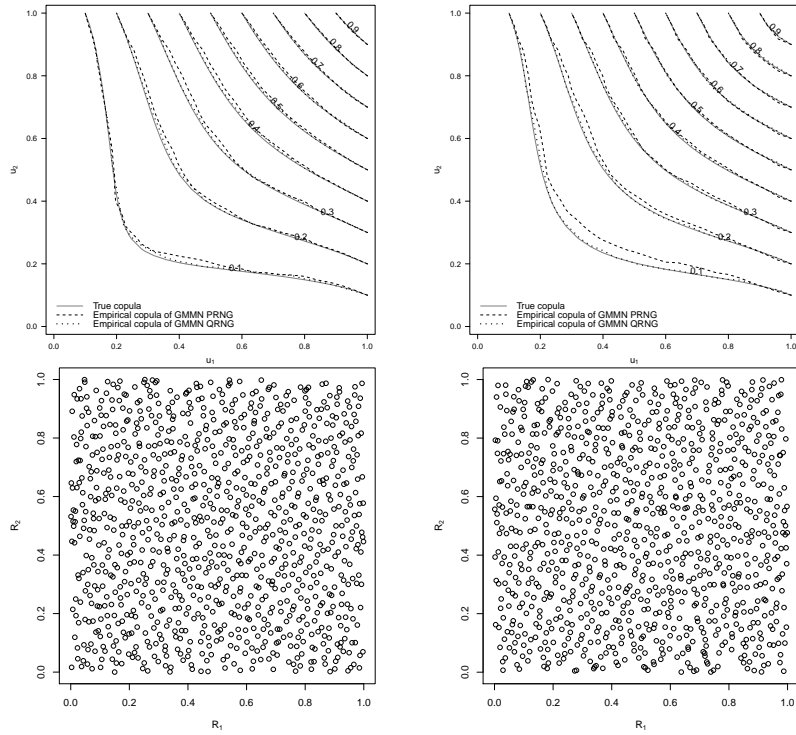


**Figure 4** Top row contains contour plots of true Clayton- $t(90)$  (left) and Gumbel- $t(90)$  (right) mixture copulas along with the corresponding contour plots of empirical copulas based on GMMN PRNG and GMMN QRNG samples of size  $n_{\text{gen}} = 1000$ . Bottom row contains Rosenblatt-transformed GMMN QRNG samples corresponding to the same mixture copulas.

demonstrate the ability of GMMNs to capture such dependence structures, we consider the simplest three-dimensional copula for visualization and investigate higher-dimensional NACs in Sections 3.3 and 4. The three-dimensional NAC we consider here is

$$C(\mathbf{u}) = C_0(C_1(u_1, u_2), u_3), \quad \mathbf{u} \in [0, 1]^3, \quad (10)$$

where  $C_0$  is a Clayton copula with  $\tau_0 = 0.25$  and  $C_1$  is a Clayton copula with  $\tau_1 = 0.50$ . In Sections 3.3 and 4, we will present examples of five- and ten-dimensional NACs.

Bivariate Marshall–Olkin copulas are of the form

$$C(u_1, u_2) = \min\{u_1^{\alpha_1}u_2, u_1u_2^{1-\alpha_2}\}, \quad u_1, u_2 \in [0, 1],$$

where  $\alpha_1, \alpha_2 \in [0, 1]$ . A notable feature of Marshall–Olkin copulas is that they have both an absolutely continuous component and a singular component. In particular, the singular component is determined by all points which satisfy  $u_1^{\alpha_1} = u_2^{\alpha_2}$ . Accurately capturing this singular component presents a different challenge for GMMNs, which is why we included this copula despite the fact that there also exists a QRNG via the inverse Rosenblatt transform for this copula; see Cambou et al. (2017). As an example for visual assessment, we consider a Marshall–Olkin copula with  $\alpha_1 = 0.75$  and  $\alpha_2 = 0.60$ .

We also consider three mixture models all of which are equally weighted two-component mixture copulas with one component being a 90-degree-rotated  $t_4$  copula with  $\tau = 0.50$ . The first two models are the Clayton- $t(90)$  and Gumbel- $t(90)$  mixture copulas as previously introduced. The second component in the third model is a Marshall–Olkin copula with parameters  $\alpha_1 = 0.75$  and  $\alpha_2 = 0.60$ . We refer to this third model as the MO- $t(90)$  copula.

Figures 5–7 display PRNG samples (left column) from a (2, 1)-nested Clayton copula as in (10), a MO copula, and the three mixture copulas, respectively, along with GMMN PRNG samples (middle column) and GMMN QRNG samples (right column) corresponding to each copula  $C$ . The similarity between the GMMN PRNG samples in the middle column plot(s) and the PRNG samples in the left column plot(s) indicate that the copulas  $C$  were learned sufficiently well by their corresponding GMMNs. Note that in the case of the nested Clayton copula example, we can only comment on how well the bivariate margins of the copula  $C$  were learned. From the right column plots, we can mainly observe that the GMMN QRNG samples contain less gaps and clusters when compared with the corresponding PRNG and GMMN PRNG samples. The fact that GMMNs were capable of learning the main features, including the singular components, of the MO copula and the MO- $t(90)$  mixture copula is particularly noteworthy given how hard it is to even visually learn a distribution well.

### 3.3 Assessment of GMMN samples by the Cramér-von Mises statistic

After a purely visual inspection of the generated samples, we now assess the quality of GMMN PRNG and GMMN QRNG samples more formally with the help of a goodness-of-fit statistic. Since bivariate copulas have been investigated in detail in the previous section, we focus on higher-dimensional copulas in this section.

### 3 GMMN PRNGs and QRNGs for copula models

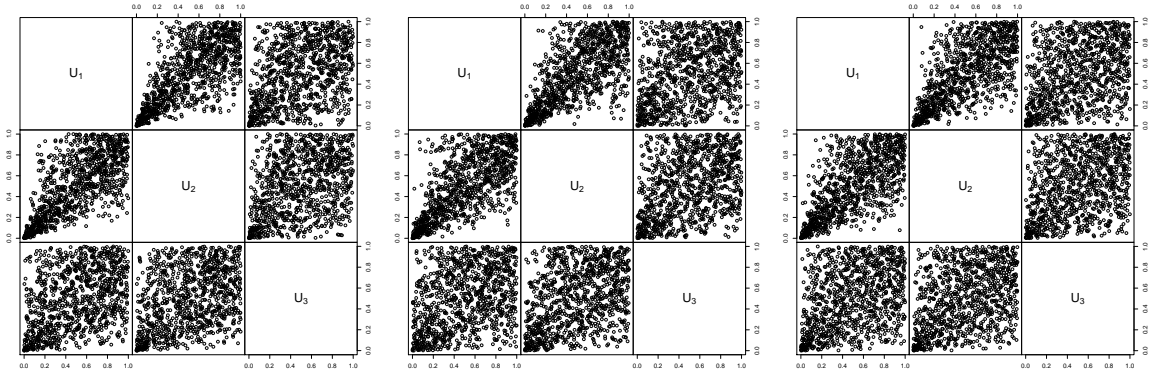


**Figure 5** PRNG (left), GMMN PRNG (middle) and GMMN QRNG (right) samples of size  $n_{\text{gen}} = 1000$  from a  $(2,1)$ -nested Clayton copula (as in (10)) with  $\tau_0 = 0.25$  and  $\tau_1 = 0.50$ .

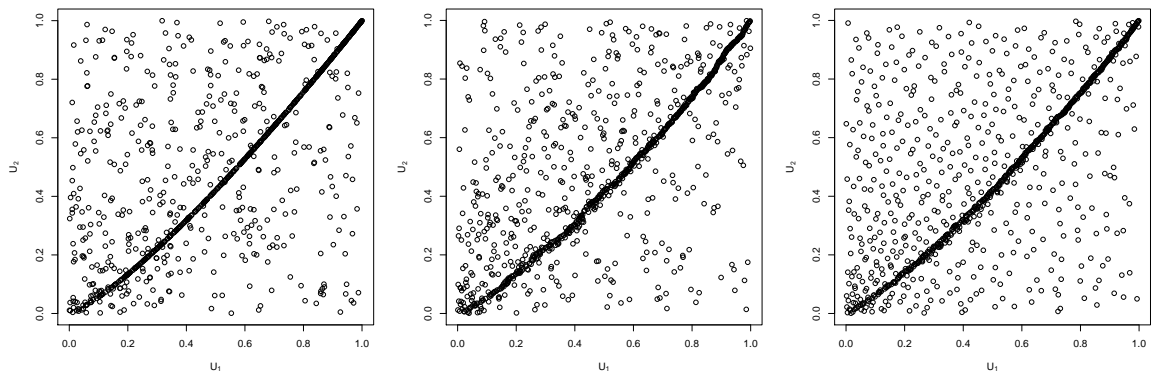


**Figure 6** PRNG (left), GMMN PRNG (middle) and GMMN QRNG (right) samples of size  $n_{\text{gen}} = 1000$  from a Marshall–Olkin copula with  $\alpha_1 = 0.75$  and  $\alpha_2 = 0.60$  (Kendall’s tau equals 0.5).

### 3 GMMN PRNGs and QRNGs for copula models

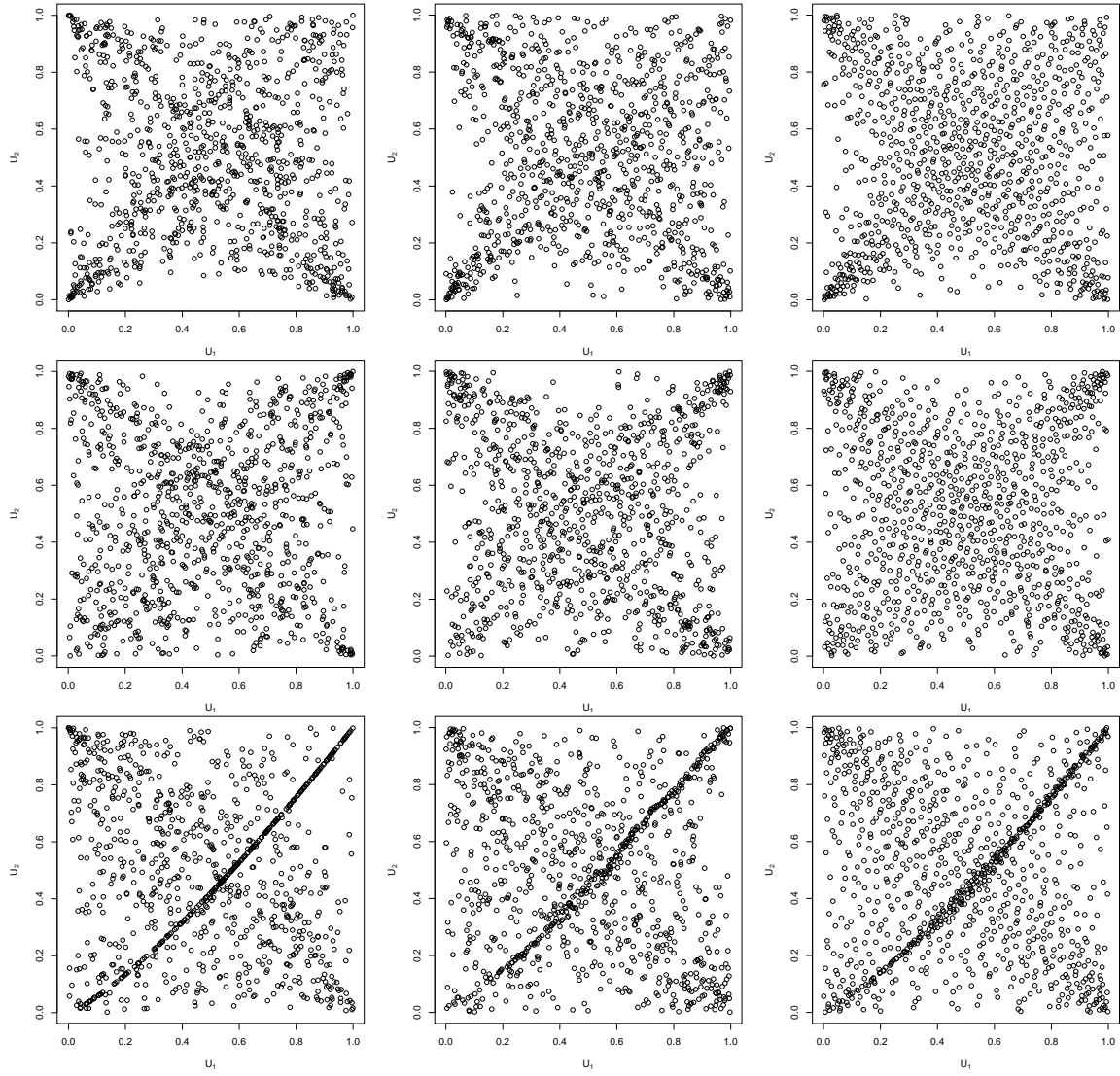


**Figure 7** PRNG (left column), GMMN PRNG (middle column) and GMMN QRNG (right column) samples of size  $n_{\text{gen}} = 1000$  from a Clayton- $t(90)$  (top row), Gumbel- $t(90)$  (middle row) and a MO- $t(90)$  mixture (bottom row) copula.

### 3 GMMN PRNGs and QRNGs for copula models

Specifically, we use the Cramér–von Mises statistic Genest et al. (2009),

$$S_{n_{\text{gen}}} = \int_{[0,1]^d} n_{\text{gen}} (C_{n_{\text{gen}}}(\mathbf{u}) - C(\mathbf{u}))^2 dC_{n_{\text{gen}}}(\mathbf{u}),$$

where the empirical copula

$$C_{n_{\text{gen}}}(\mathbf{u}) = \frac{1}{n_{\text{gen}}} \sum_{i=1}^{n_{\text{gen}}} \mathbb{1}\{\hat{U}_{i1} \leq u_1, \dots, \hat{U}_{id} \leq u_d\}, \quad \mathbf{u} \in [0, 1]^d,$$

is the distribution function of the pseudo-observations. For each copula  $C$ , we compute realizations of  $S_{n_{\text{gen}}}$  three times – once for the case where  $\hat{U}_i$ ,  $i = 1, \dots, n_{\text{gen}}$ , are the pseudo-observations obtained from a sample of the true copula under consideration (as a benchmark), once for the case where they are the (post-processed) GMMN PRNG samples and once for the case where they are the (post-processed) GMMN QRNG samples.

For each copula considered, we fix  $n_{\text{gen}} = 1000$  and compute  $B = 100$  realizations of  $S_{n_{\text{gen}}}$  based on pseudo-observations from PRNG samples directly from the copula under consideration, GMMN PRNG and GMMN QRNG samples as described. We then use box plots to depict the distribution of  $S_{n_{\text{gen}}}$  in each case. Figure 8 displays these box plots for  $t_4$  (top row), Clayton (middle row) and Gumbel (bottom row) copulas of dimensions  $d = 5$  (left column),  $d = 10$  (right column) and  $\tau = 0.50$ . Similarly, Figure 9 displays such box plots for  $d$ -dimensional nested Clayton (left column) and nested Gumbel (right column) copulas for  $d = 3$  (top row),  $d = 5$  (middle row) and  $d = 10$  (bottom row). The three-dimensional NACs have a structure as in (10) with  $\tau_0 = 0.25$  and  $\tau_1 = 0.50$ , the five-dimensional NACs have structure  $C_0(C_1(u_1, u_2), C_2(u_3, u_4, u_5))$  with corresponding  $\tau_0 = 0.25$ ,  $\tau_1 = 0.50$  and  $\tau_2 = 0.75$ , and the ten-dimensional NACs have structure  $C_0(C_1(u_1, \dots, u_5), C_2(u_6, \dots, u_{10}))$  with corresponding  $\tau_0 = 0.25$ ,  $\tau_1 = 0.50$  and  $\tau_2 = 0.75$ .

We can observe from both figures that the distribution of  $S_{n_{\text{gen}}}$  based on the GMMN PRNG samples and copula PRNG samples are similar, with slightly higher  $S_{n_{\text{gen}}}$  values for the GMMN PRNG samples, especially for  $d = 10$ . Overall, the (pseudo-observations of the) GMMN PRNG samples approximate the (pseudo-observations of the) copula PRNG samples quite well according to these assessments.

Additionally, we can observe that the distribution of  $S_{n_{\text{gen}}}$  based on the GMMN QRNG samples is closer to zero than the distribution based on the GMMN PRNG samples. This provides some evidence that the low-discrepancy of input RQMC points sets has been preserved under the respective (trained) GMMN transforms.

We also see that  $S_{n_{\text{gen}}}$  values based on the GMMN QRNG samples are clearly lower than  $S_{n_{\text{gen}}}$  values based on the copula PRNG samples, with the exception of (some) copulas with  $d = 10$  where the distributions of  $S_{n_{\text{gen}}}$  are more similar. These observations provide some indication that GMMN RQMC estimators should outperform MC estimators constructed using PRNG samples from  $C$ . We investigate this comparison thoroughly in Section 4.

### 3 GMMN PRNGs and QRNGs for copula models

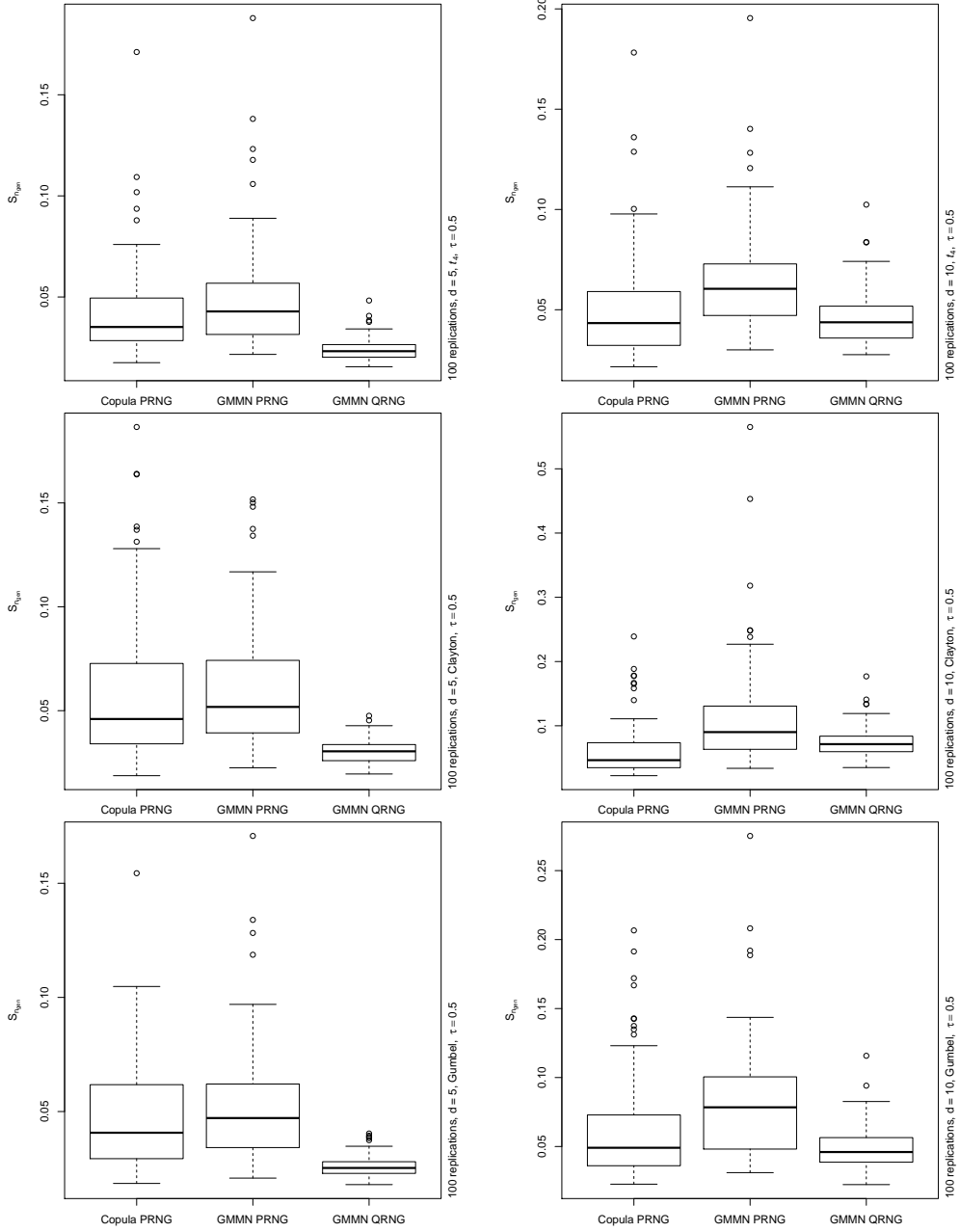


**Figure 8** Box plots based on  $B = 100$  realization of  $S_{n_{\text{gen}}}$  computed from pseudo-observations of a pseudo-sample of size  $n_{\text{gen}} = 1000$  of the true underlying copula (denoted by Copula PRNG), from pseudo-observations of GMMN PRNG samples (denoted by GMMN PRNG) and from pseudo-observations of GMMN QRNG samples (denoted by GMMN QRNG) for a  $t_4$  (top row), Clayton (middle row) and Gumbel (bottom row) copula with  $\tau = 0.5$  as well as  $d = 5$  (left column) and  $d = 10$  (right column).

### 3 GMMN PRNGs and QRNGs for copula models

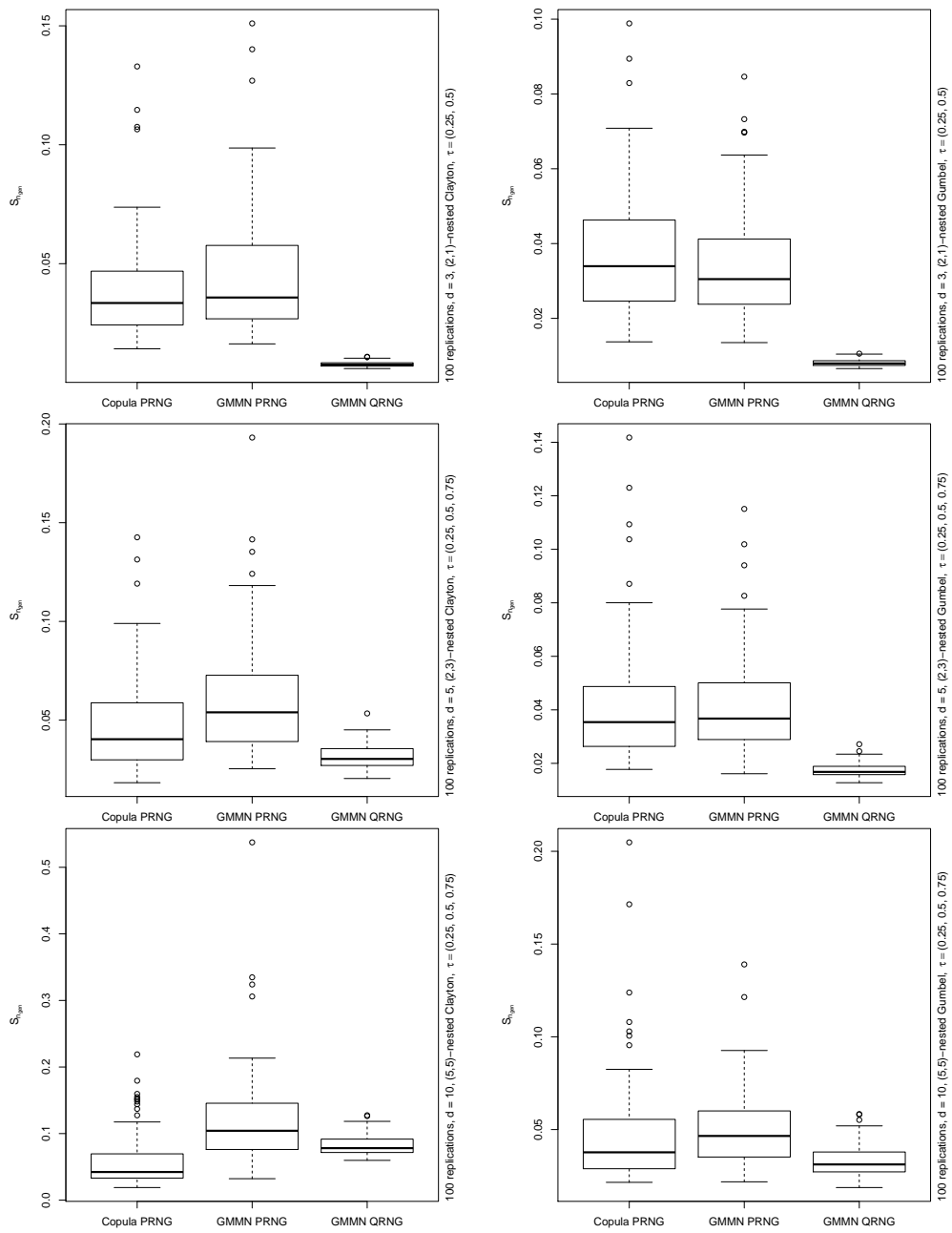


**Figure 9** As in Figure 8 but for nested Clayton (left column) and nested Gumbel (right column) copulas and for  $d = 3$  (top row),  $d = 5$  (middle row) and  $d = 10$  (bottom row).

## 4 Application of quasi-random GMMN sampling

In this section we numerically investigate the variance-reduction properties of the GMMN RQMC estimator  $\mu_{n_{\text{gen}}}$  in (7) for various functions  $\Psi$  and transforms  $q = f_{\hat{\theta}} \circ \Phi^{-1}$  corresponding to different copulas  $C$ . Where possible, we compare  $\mu_{n_{\text{gen}}}$  with estimators arising from standard copula PRNGs and QRNGs; see Cambou et al. (2017). However, note that the QRNGs in the latter reference are only applicable to some of the copulas we consider here. We consider two categories of functions  $\Psi$ . The first category consists of two *test functions* which are primarily used to test the performance of  $\mu_{n_{\text{gen}}}$  in terms of its ability to preserve the low discrepancy of  $\tilde{P}_{n_{\text{gen}}}$ . For this category of functions, we plot median absolute deviation estimates of the GMMN RQMC and other estimators to compare their convergence rate. The second category of functions are motivated from practical applications in risk management. For this category of functions, standard deviation estimates will be computed to compare their convergence rate. Note that the theoretical convergence rates of the Monte Carlo (MC) estimator's absolute deviation and standard deviation are of the order  $O(n_{\text{gen}}^{-0.5})$ .

Standard deviation and median absolute deviation estimates will be computed based on  $B = 25$  randomized point sets  $\tilde{P}_{n_{\text{gen}}}$  for each of  $n_{\text{gen}} \in \{2^9, 2^{9.5}, \dots, 2^{18}\}$  to help roughly gauge the convergence rate for all estimators. Furthermore, regression coefficients  $\alpha$  (obtained by regressing the logarithm of the measure of interest on the logarithm of  $n_{\text{gen}}$ ) are computed and displayed to allow for an easy comparison of the corresponding convergence rates  $O(n_{\text{gen}}^{-\alpha})$ .

### 4.1 Test functions

The first test function we consider is

$$\Psi_1(\mathbf{U}) = \frac{3}{d} \sum_{j=1}^d U_j^2.$$

Notice that  $\mathbb{E}(\Psi_1(\mathbf{U})) = 1$  for  $\mathbf{U} \sim C$  from any copula  $C$ . For experiments involving this test function we thus do not perform the post-processing step of building pseudo-observations of the GMMN output.

Figure 10 shows plots of median absolute deviation estimates for estimating  $\mathbb{E}(\Psi_1(\mathbf{U}))$  for  $t_4$  (first row), Clayton (second row) and Gumbel (third row) copulas in dimensions  $d = 2$  (left column),  $d = 5$  (middle column) and  $d = 10$  (right column), as well as nested Gumbel copulas (fourth row) in dimension  $d = 3$  (left column),  $d = 5$  (middle column) and  $d = 10$  (right column), with hierarchical structure and parameterization as described in Section 3.3. For the  $t_4$  and Clayton copulas we numerically compare the efficiency of the GMMN RQMC estimator (with legend label “GMMN QRNG”) with the copula RQMC estimator based on the CDM method (with legend label “Copula QRNG”) and the MC estimator (with legend label “Copula PRNG”). For the Gumbel and nested Gumbel copulas, however, the CDM approach (“Copula QRNG”) is not available. The legend of each plot

## 4 Application of quasi-random GMMN sampling

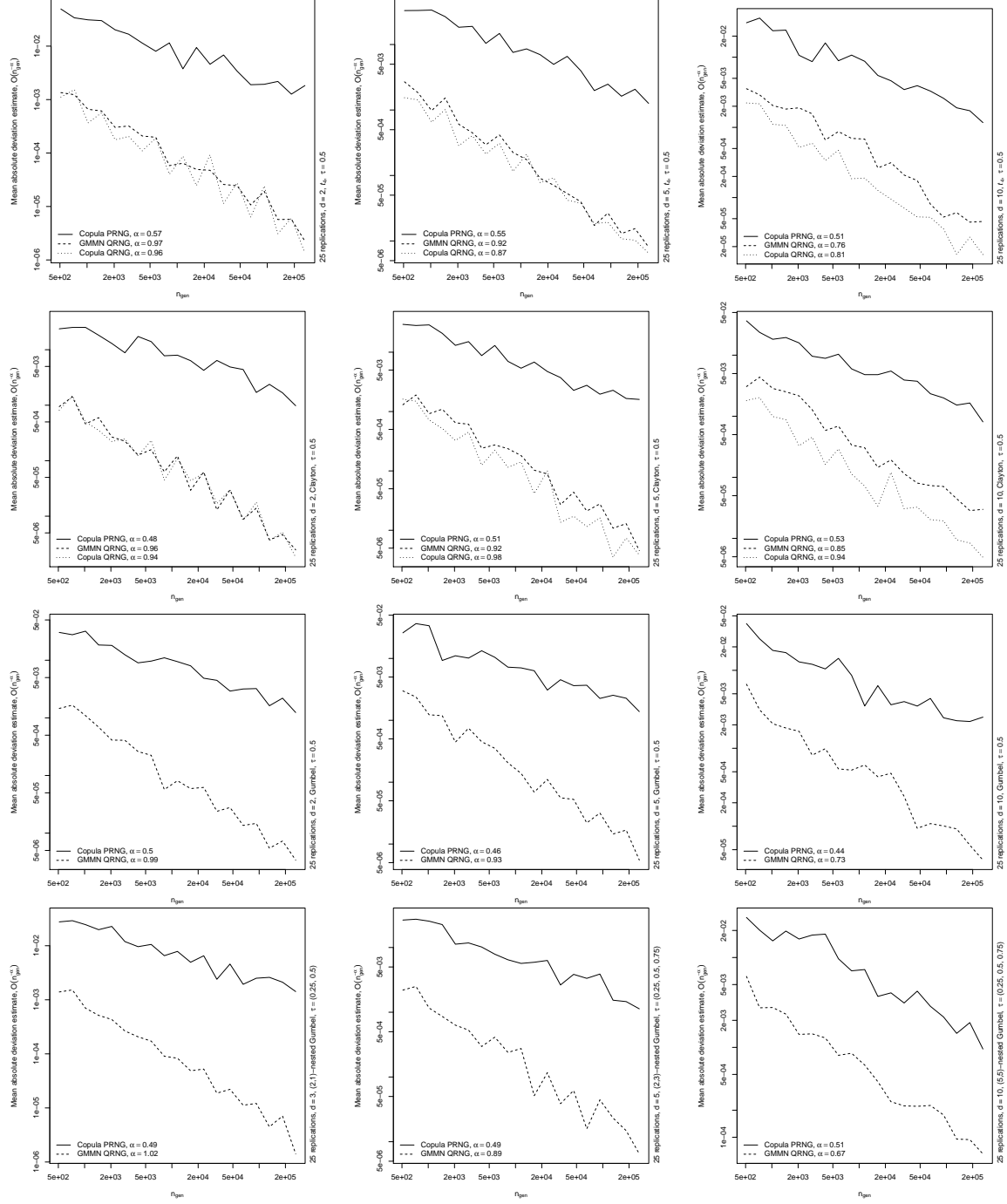


**Figure 10** Median absolute deviation estimates based on  $B = 25$  replications for estimating  $\mathbb{E}(\Psi_1(\mathbf{U}))$  via MC based on a PRNG, via the copula RQMC estimator (whenever available; rows 1–2 only) and via the GMMN RQMC estimator. Note that in rows 1–3,  $d \in \{2, 5, 10\}$ , whereas in row 4,  $d \in \{3, 5, 10\}$ .

also provides the corresponding regression coefficient  $\alpha$  which indicates the convergence rate of each estimator.

From Figure 10, we observe that the GMMN RQMC estimator clearly outperforms the MC estimator. Naturally, so does the copula RQMC estimator for the copulas for which it is available. On the one hand, the rate of convergence of the GMMN RQMC estimator reduces with increasing copula dimensions; see also the regression coefficients  $\alpha$  which decrease from 1 to approximately 0.75 when we compare the two- and ten-dimensional copulas. On the other hand, the GMMN RQMC estimator still outperforms the MC estimator.

The second test function we consider involves the Rosenblatt transform and is given by

$$\Psi_2(\mathbf{U}) = \prod_{j=1}^d \frac{|4R_j - 1| + j}{1 + j},$$

where  $R_1 = U_1$  and, for  $j = 2, \dots, d$  and if  $\mathbf{U} \sim C$ ,  $R_j = C_{j|1, \dots, j-1}(U_j | U_{j-1}, \dots, U_1)$  denotes the conditional distribution function of  $U_j$  given  $U_1 = u_1, \dots, U_{j-1} = u_{j-1}$ .

Figure 11 shows plots of median absolute deviation estimates for estimating  $\mathbb{E}(\Psi_2(\mathbf{U}))$  for  $t_4$  copulas (top row), Clayton (middle row) and Gumbel (bottom row) copulas in dimensions  $d = 2$  (left column),  $d = 5$  (middle column) and  $d = 10$  (right column). Note that we cannot apply the transform  $\Psi_2(\mathbf{U})$  for  $\mathbf{U}$  following nested Gumbel copulas as  $R_2, \dots, R_d$  are not available in this case. Overall, we observe the same pattern as for the results obtained for  $\Psi_1$ ; see Figure 10. Although the reduction in convergence rate as the copula dimension increases is more severe for  $\Psi_2$  than it is for  $\Psi_1$ , the GMMN RQMC estimator still outperforms the MC estimator.

## 4.2 Examples from risk management practice

Consider modeling the dependence of  $d$  risk-factor changes (for example, logarithmic returns) of a portfolio; see McNeil et al. (2015, Chapters 2, 6 and 7). We will demonstrate the efficiency of our GMMN RQMC estimator by considering two functionals: the joint exceedance probability of all  $d$  risk-factor changes over a threshold and the expected shortfall of the aggregate loss, that is, computing a risk measure based on the sum of all risk-factor changes.

For the first example, we focus solely on dependence models for the random vector  $\mathbf{U} = (U_1, \dots, U_d)$  following the underlying copula. The joint exceedance probability of  $(0.99, \dots, 0.99)$  is given by

$$\mathbb{P}(U_1 > 0.99, \dots, U_d > 0.99) = \mathbb{E}(\mathbb{1}\{U_1 > 0.99, \dots, U_d > 0.99\}) = \mathbb{E}(\Psi_3(\mathbf{U})),$$

for  $\Psi_3(\mathbf{u}) = \mathbb{1}\{u_1 > 0.99, \dots, u_d > 0.99\}$ . Computing such exceedance probabilities is of interest, for example, for quantifying the probability of joint losses of the  $d$  (dependent) components of the portfolio.

Figure 12 shows plots of standard deviation estimates for estimating  $\mathbb{E}(\Psi_3(\mathbf{U}))$  for the same set of copulas considered in Figure 10. We can observe from the plots that the GMMN

## 4 Application of quasi-random GMMN sampling

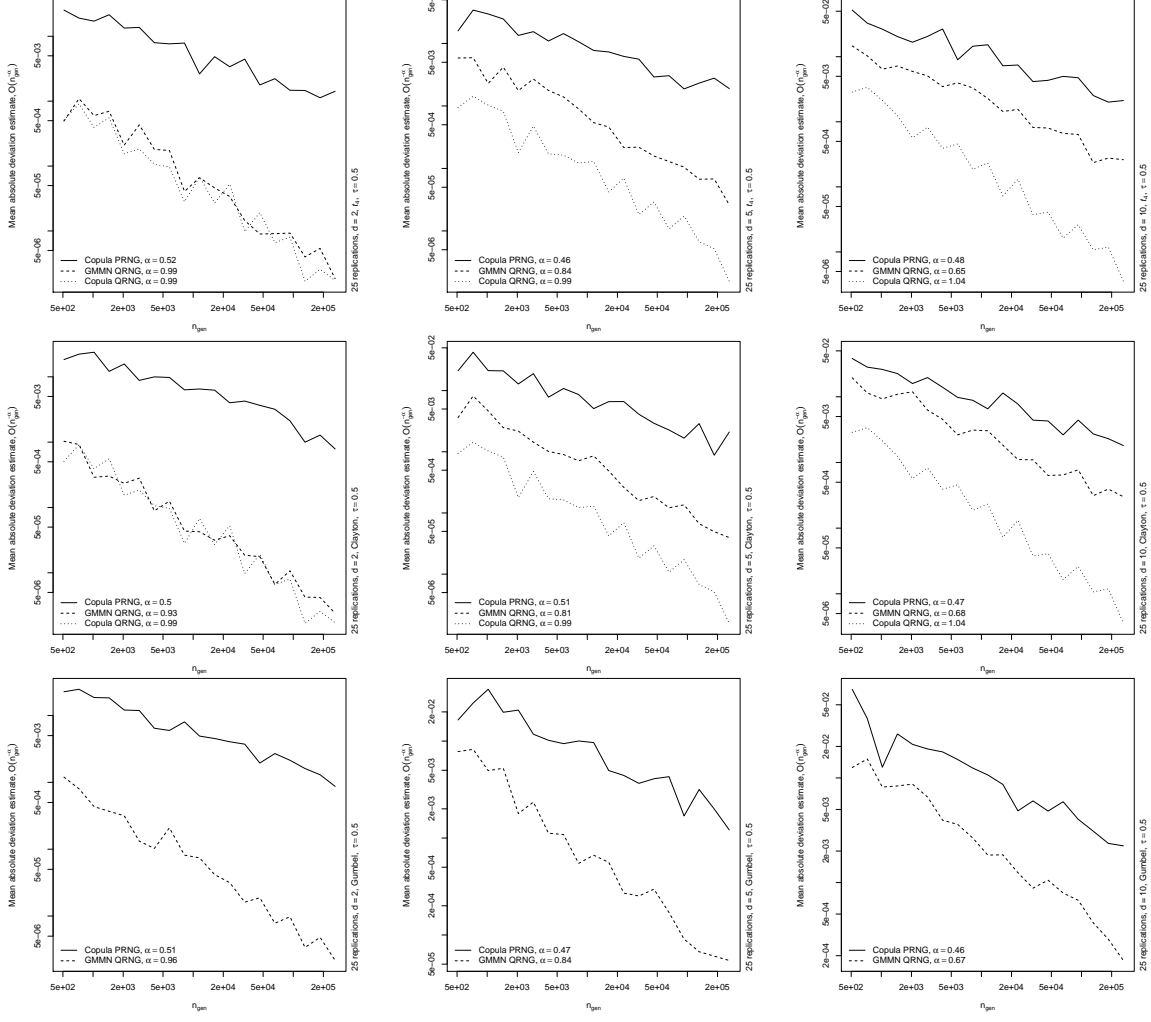


**Figure 11** Median absolute deviation estimates based on  $B = 25$  replications for estimating  $\mathbb{E}(\Psi_2(\mathbf{U}))$  via MC based on a PRNG, via the copula RQMC estimator (whenever available; rows 1–2 only) and via the GMMN RQMC estimator. Note that in rows 1–3,  $d \in \{2, 5, 10\}$ .

## 4 Application of quasi-random GMMN sampling

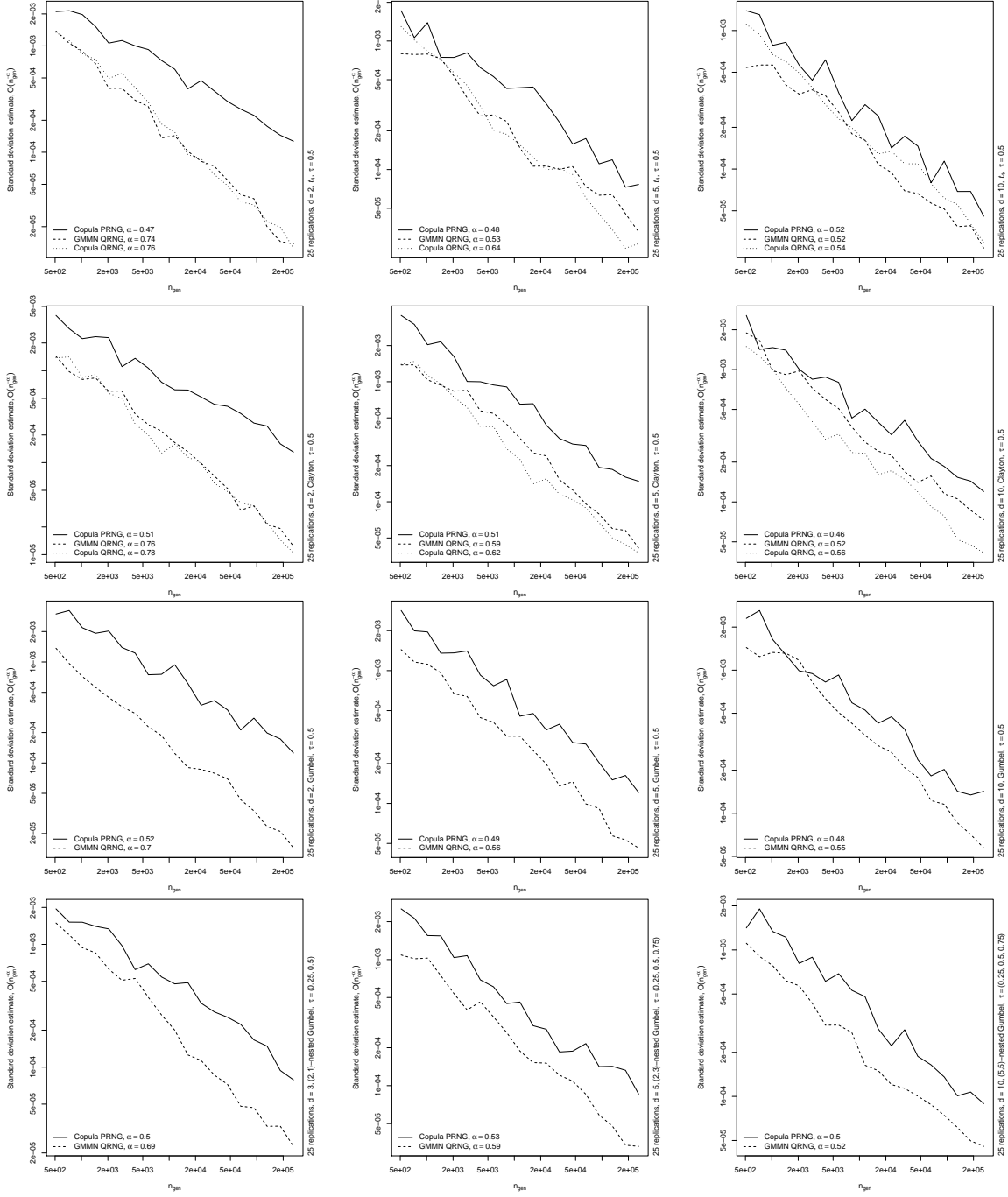


**Figure 12** Standard deviation estimates based on  $B = 25$  replications for estimating  $\mathbb{E}(\Psi_3(\mathbf{U}))$  via MC based on a PRNG, via the copula RQMC (whenever available; rows 1–2 only) and via the GMMN RQMC estimator. Note that in rows 1–3,  $d \in \{2, 5, 10\}$ , whereas in row 4,  $d \in \{3, 5, 10\}$ .

## 5 Discussion

RQMC estimator outperforms the MC estimator. Similar to  $\mathbb{E}(\Psi_1(\mathbf{U}))$  and  $\mathbb{E}(\Psi_2(\mathbf{U}))$ , we see a decrease in the convergence rate of the GMMN RQMC estimator as the copula dimension increases, although the latter still outperforms the MC estimator.

Now consider expected shortfall, a popular risk measure in quantitative risk management practice. If  $\mathbf{X} = (X_1, \dots, X_d)$  denotes a random vector of risk-factor changes with  $N(0, 1)$  margins,  $S = \sum_{j=1}^d X_j$  is the aggregate loss. The expected shortfall at level 0.99 of  $S$  is given by

$$\frac{1}{1 - 0.99} \int_{0.99}^1 F_S^{-1}(u) du = \mathbb{E}(S \mid S > F_S^{-1}(0.99)) = \mathbb{E}(\Psi_4(\mathbf{X})),$$

where  $F_S^{-1}$  denotes the quantile function of  $S$ . As done previously, various copulas will be used to model the dependence between the components of  $\mathbf{X}$ .

Figure 13 shows plots of standard deviation estimates for estimating  $\mathbb{E}(\Psi_4(\mathbf{X}))$  for the same copula models as considered before. We can observe from the plots that the GMMN RQMC estimator outperforms the MC estimator. Similar as before, we see a decrease in the convergence rate of the GMMN RQMC estimator as the copula dimension increases, although the latter still outperforms the MC estimator.

## 5 Discussion

This work has been inspired by the simple question of how one can construct a quasi-random number generator for a large variety of multivariate distributions. Until recently, this was only possible for a few multivariate distributions with specific underlying copulas. In general, for the vast majority of multivariate distributions, constructing quasi-random number generators is a hard problem Cambou et al. (2017). Our approach based on GMMNs provides a first universal approach for building quasi-random number generators for such distributions. It is generally difficult to assess the low-discrepancy property of (non-uniform) quasi-random samples; thus, to evaluate the quality of our GMMN QRNG samples, we focus on their variance reduction effects when used to estimate  $\mathbb{E}(\Psi(\mathbf{X}))$ .

However, this does not mean that the problem is completely solved. Our approach depends on first learning a generator  $f_{\hat{\theta}}$  such that, given  $\mathbf{Z}$  (from some known distribution such as the multivariate uniform or standard normal),  $f_{\hat{\theta}}(\mathbf{Z})$  follows the targeted multivariate distribution. Conditional on this first step being successful, we can then replace  $\mathbf{Z}$  with  $F_{\mathbf{Z}}^{-1}(\tilde{\mathbf{v}})$  to generate quasi-random samples.

In high dimensions, however, learning an entire distribution is a hard problem, and so is learning the generator  $f_{\hat{\theta}}$ . At a superficial level, the literature on generative NNs – and the many headlines covering them – may give the impression that such NNs are now capable of generating samples from very high-dimensional distributions. This, of course, is not true; see, for example, Arjovsky et al. (2017), Arora, Risteski, et al. (2018), and Tolstikhin et al. (2017). In particular, while available evidence is convincing that any *specific* generated sample  $f_{\hat{\theta}}(\mathbf{Z}_0)$ , typically an image, can be very realistic in the sense that it looks just like a

## 5 Discussion

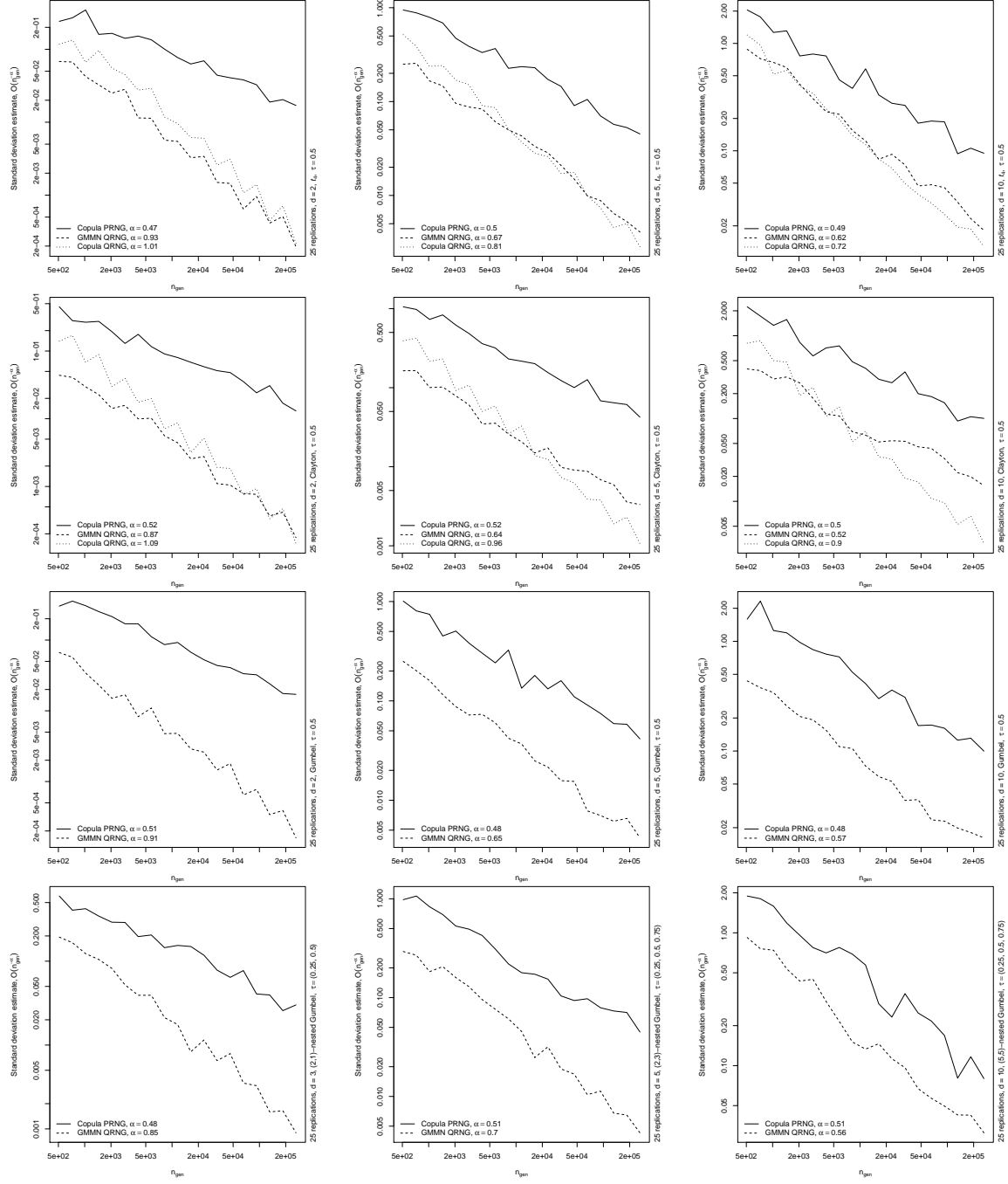


**Figure 13** Standard deviation estimates based on  $B = 25$  replications for estimating  $\mathbb{E}(\Psi_4(\mathbf{X}))$  via MC based on a PRNG, via the copula RQMC (whenever available; rows 1–2 only) and via the GMMN RQMC estimator. Note that in rows 1–3,  $d \in \{2, 5, 10\}$ , whereas in row 4,  $d \in \{3, 5, 10\}$ .

typical training sample, this is not the same as saying that the *entire collection* of generated samples  $\{f_{\hat{\theta}}(\mathbf{Z}_1), f_{\hat{\theta}}(\mathbf{Z}_2), \dots\}$  will have the same distribution as the training sample.

Unlike widely cited generative NNs such as variational autoencoders and generative adversarial networks, GMMNs are capable of learning entire distributions, because they rely on the MMD-criterion rather than some other criteria, for example, mean squared error, that do not measure the discrepancy between entire distributions. Even so, this still does not mean GMMNs are practical for very high dimensions yet, simply because the fundamental curse of dimensionality cannot be avoided easily. At the moment, it is simply not realistic to hope that one can learn an entire distribution in high dimensions from a training sample of only moderate size, but, as we have noted earlier, the effectiveness of GMMNs depends critically on the batch size  $n_{\text{bat}}$  used to train them. That is, increasing  $n_{\text{bat}}$  will lead to better training of the GMMNs at the expense of quadratically increasing memory requirements.

Going forward there are two primary impediments to the construction of quasi-random number generators for higher-dimensional copulas and distributions. Firstly, the problem of distribution learning via generative NNs remains a challenging task in higher dimensions. We may also consider using other goodness-of-fit statistics for multivariate distributions rather than the MMD as the loss function (provided that the statistic is differentiable in order to train a generative NN). Secondly, we discovered from our empirical investigation in Section 4 that the convergence rates of GMMN RQMC estimators decrease with increasing dimension. Preserving the low-discrepancy of RQMC point sets upon transformations in high dimensions remains an open challenge in this regard.

The reason why in this paper we have focused on dependence structures described via known and fixed parametric copula models (or mixtures thereof) is because that's the only way for us to statistically assess the performance of our GMMN QRNG samples, but we emphasize that the key feature of our method is that, given a relatively large data set with dependence structures not well described by any parametric copula model, we are now able to generate quasi-random samples from its empirical distribution.

## A Analyzing GMMN QMC and GMMN RQMC estimators

### A.1 QMC point sets

The idea behind QRNGs is to replace pseudo- $U(0, 1)^p$  random numbers with low-discrepancy points sets  $P_{n_{\text{gen}}}$  to produce a more homogeneous coverage of  $[0, 1]^p$  in comparison to PRNGs. That is, with respect to a certain *discrepancy measure*, the empirical distribution of the  $P_{n_{\text{gen}}}$  is closer to the uniform distribution  $U(0, 1)^p$  than samples drawn using PRNGs.

Established notions of the discrepancy of a point set  $P_{n_{\text{gen}}}$  are as follows. The *discrepancy function* of  $P_{n_{\text{gen}}}$  in an interval  $I = [\mathbf{0}, \mathbf{b}] = \prod_{j=1}^p [0, b_j]$ ,  $b_j \in (0, 1]$ ,  $j = 1, \dots, p$ , is defined

by

$$D(I; P_{n_{\text{gen}}}) = \frac{1}{n_{\text{gen}}} \sum_{i=1}^{n_{\text{gen}}} \mathbb{1}_{\{\mathbf{v}_i \in I\}} - \lambda(I),$$

where  $\lambda(I)$  is the  $p$ -dimensional Lebesgue measure of  $I$ . Thus the discrepancy function is the difference between the number of points of  $P_{n_{\text{gen}}}$  in  $I$  and the probability of a  $p$ -dimensional standard uniform random vector to fall in  $I$ . For  $\mathcal{A} = \{[\mathbf{0}, \mathbf{b}) : \mathbf{b} \in (0, 1]^p\}$ , the *star discrepancy* of  $P_{n_{\text{gen}}}$  is defined by

$$D^*(P_{n_{\text{gen}}}) = \sup_{I \in \mathcal{A}} |D(I; P_{n_{\text{gen}}})|.$$

If  $P_{n_{\text{gen}}}$  satisfies the condition  $D^*(P_{n_{\text{gen}}}) \in O(n_{\text{gen}}^{-1} (\log n_{\text{gen}})^p)$ , it is called a *low-discrepancy sequence* Lemieux (2009, p. 143).

There are different approaches to construct (deterministic) low-discrepancy sequences; see Lemieux (2009, Chapters 5–6). The two main approaches involve either lattices (grids which behave well under projections) or digital nets/sequences. In our numerical investigations presented in Sections 3–4, we worked with a type of digital net constructed using the Sobol' sequence; see Sobol' (1967).

## A.2 Analyzing the GMMN QMC estimator

In this section, we will derive conditions under which the (non-randomized) GMMN QMC estimator

$$\frac{1}{n_{\text{gen}}} \sum_{i=1}^{n_{\text{gen}}} \Psi(q(\mathbf{v}_i)) = \frac{1}{n_{\text{gen}}} \sum_{i=1}^{n_{\text{gen}}} h(\mathbf{v}_i),$$

where  $q = f_{\hat{\theta}} \circ F_{\mathbf{Z}}^{-1}$  and  $h = \Psi \circ q = \Psi \circ f_{\hat{\theta}} \circ F_{\mathbf{Z}}^{-1}$ , has a small error when approximating  $\mathbb{E}(\Psi(\mathbf{Y}))$ . In the following analysis, we need to further assume that  $\text{supp}(F_{\mathbf{X}})$  and  $\text{supp}(F_{\mathbf{Y}})$  are bounded.

The *Koksma–Hlawka inequality* Niederreiter (1992) for a function  $g : [0, 1]^p \rightarrow \mathbb{R}$  says that

$$\left| \frac{1}{n_{\text{gen}}} \sum_{i=1}^{n_{\text{gen}}} g(\mathbf{v}_i) - \mathbb{E}(g(\mathbf{U}')) \right| \leq V(g) D^*(P_{n_{\text{gen}}}),$$

where  $\mathbf{U}' \sim \text{U}(0, 1)^p$  and the variation  $V(g)$  is understood in the sense of Hardy and Krause; we refer to the right-hand side of the inequality as *Koksma–Hlawka bound*. From this Koksma–Hlawka inequality, we can establish that if  $g$  has finite bounded variation, that is  $V(g) < \infty$ , then the convergence rate for  $\frac{1}{n_{\text{gen}}} \sum_{i=1}^{n_{\text{gen}}} g(\mathbf{v}_i)$  is determined by  $D^*(P_{n_{\text{gen}}}) = O(n_{\text{gen}}^{-1} (\log n_{\text{gen}})^p)$ .

We can use the Koksma–Hlawka inequality to analyze the convergence of the GMMN QMC estimator  $\frac{1}{n_{\text{gen}}} \sum_{i=1}^{n_{\text{gen}}} \Psi(\mathbf{y}_i)$  of  $\mathbb{E}(\Psi(\mathbf{Y}))$ , where  $\mathbf{y}_i = q(\mathbf{v}_i)$ ,  $i = 1, \dots, n_{\text{gen}}$  and  $\mathbf{Y} \sim F_{\mathbf{Y}}$ , by establishing the conditions under which  $V(h)$  is bounded. To that end, consider the following proposition.

**Proposition A.1 (Sufficient conditions for finiteness of the Koksma–Hlawka bound)**

Assume that  $\text{supp}(F_{\mathbf{Y}})$  is bounded and all appearing partial derivatives of  $q$  and  $\Psi$  exist and are continuous. Consider  $q = f_{\hat{\theta}} \circ F_{\mathbf{Z}}^{-1}$ , the point set  $P_{n_{\text{gen}}} = \{\mathbf{v}_1, \dots, \mathbf{v}_{n_{\text{gen}}}\} \subseteq [0, 1]^p$  and let  $\mathbf{y}_i = q(\mathbf{v}_i)$ ,  $i = 1, \dots, n_{\text{gen}}$ , denote the GMMN QRNG sample. Suppose that

- 1)  $\Psi(\mathbf{y}) < \infty$  for all  $\mathbf{y} \in \text{supp}(F_{\mathbf{Y}})$  and

$$\frac{\partial^{|\beta|_1} \Psi(\mathbf{y})}{\partial^{\beta_1} y_1 \dots \partial^{\beta_d} y_d} < \infty, \quad \mathbf{y} \in \text{supp}(F_{\mathbf{Y}}),$$

for all  $\beta = (\beta_1, \dots, \beta_d) \subseteq \{0, \dots, d\}^d$  and  $|\beta|_1 = \sum_{j=1}^d \beta_j \leq d$ ;

- 2) there exists an  $M > 0$  such that  $|D^k F_{Z_j}^{-1}| \leq M$ , for each  $k, j = 1, \dots, p$ , where  $D^k$  denotes the  $k$ -fold derivative of its argument;
- 3) there exists, for each layer  $l = 1, \dots, L+1$  of the NN  $f_{\hat{\theta}}$ , an  $N_l > 0$  such that  $|D^k \phi_l| \leq N_l$  for all  $k = 1, \dots, p$ ; and
- 4) the parameter vector  $\hat{\theta} = (\hat{W}_1, \dots, \hat{W}_{L+1}, \hat{b}_1, \dots, \hat{b}_{L+1})$  of the fitted NN is bounded.

Then there exists a constant  $c$  independent of  $n_{\text{gen}}$ , but possibly depending on  $\Psi$ ,  $\hat{\theta}$ ,  $M$  and  $N_1, \dots, N_{L+1}$ , such that

$$\left| \frac{1}{n_{\text{gen}}} \sum_{i=1}^{n_{\text{gen}}} \Psi(\mathbf{y}_i) - \mathbb{E}(\Psi(\mathbf{Y})) \right| \leq c D^*(P_{n_{\text{gen}}}).$$

*Proof.* To begin with note that for any  $q$  such that  $q(\mathbf{U}') \sim F_{\mathbf{Y}}$ , we know that  $\mathbf{Y}$  is in distribution equal to  $q(\mathbf{U}')$  and thus  $\mathbb{E}(\Psi(\mathbf{Y})) = \mathbb{E}(\Psi(q(\mathbf{U}')) = \mathbb{E}(h(\mathbf{U}'))$ . Based on this property, we can obtain the Koksma–Hlawka bound  $V(h)D^*(P_{n_{\text{gen}}})$  for the change of variable  $h$ .

Following Lemieux (2009, Section 5.6.1), we can derive an expression for  $V(h)$ . To this end, let

$$V^{(j)}(h; \boldsymbol{\alpha}) = \int_{[0,1)^j} \left| \frac{\partial^j h^{(\boldsymbol{\alpha})}(v_{\alpha_1}, \dots, v_{\alpha_j})}{\partial v_{\alpha_j} \dots \partial v_{\alpha_1}} \right| dv_{\alpha_1} \dots dv_{\alpha_j},$$

where  $h^{(\boldsymbol{\alpha})}(v_{\alpha_1}, \dots, v_{\alpha_j}) = h(\tilde{v}_1, \dots, \tilde{v}_p)$  for  $\tilde{v}_k = v_k$  if  $k \in \{\alpha_1, \dots, \alpha_j\}$  and  $\tilde{v}_k = 1$  otherwise. Then

$$V(h) = \sum_{j=1}^p \sum_{\boldsymbol{\alpha}: |\boldsymbol{\alpha}|_1=j} V^{(j)}(h; \boldsymbol{\alpha}), \tag{11}$$

where the inner sum is taken over all  $\boldsymbol{\alpha} = (\alpha_1, \dots, \alpha_j)$  with  $\{\alpha_1, \dots, \alpha_j\} \subseteq \{1, \dots, p\}$  – see also Niederreiter (1992, pp. 19–20), E. Hlawka (1961, eq. (4)) and Hlawka and Mück (1972, eq. (4')). Following Hlawka and Mück (1972) and Constantine and Savits (1996, Theorem 2.1), we then have

$$\left| \frac{\partial^j h^{(\boldsymbol{\alpha})}(v_{\alpha_1}, \dots, v_{\alpha_j})}{\partial v_{\alpha_j} \dots \partial v_{\alpha_1}} \right| = \sum_{1 \leq |\boldsymbol{\beta}|_1 \leq j} \frac{\partial^{|\boldsymbol{\beta}|_1} \Psi}{\partial^{\beta_1} y_1 \dots \partial^{\beta_d} y_d} \sum_{i=1}^j \sum_{(\boldsymbol{\kappa}, \mathbf{k}) \in \pi_i(\boldsymbol{\kappa}, \mathbf{k})} c_{\boldsymbol{\kappa}} \prod_{m=1}^i \frac{\partial^{|\boldsymbol{\kappa}_m|_1} q_{k_m}^{(\boldsymbol{\alpha})}(v_{\alpha_1}, \dots, v_{\alpha_j})}{\partial^{\kappa_{mj}} v_{\alpha_j} \dots \partial^{\kappa_{m1}} v_{\alpha_1}}, \quad (12)$$

where  $\boldsymbol{\beta} \in \mathbb{N}_0^d$  and where  $\pi_i(\boldsymbol{\kappa}, \mathbf{k})$  denotes the set of pairs  $(\boldsymbol{\kappa}, \mathbf{k})$  such that  $\mathbf{k} = (k_1, \dots, k_i) \in \{1, \dots, d\}^i$  and  $\boldsymbol{\kappa} = (\boldsymbol{\kappa}_1, \dots, \boldsymbol{\kappa}_i)$  with  $\boldsymbol{\kappa}_m = (\kappa_{m1}, \dots, \kappa_{mj}) \in \{0, 1\}^j$ ,  $m = 1, \dots, i$ , and  $\sum_{m=1}^i \kappa_{mi} = 1$  for  $i = 1, \dots, j$ ; see Constantine and Savits (1996) for more details on  $\pi_i(\boldsymbol{\kappa}, \mathbf{k})$  and the constants  $c_{\boldsymbol{\kappa}}$ . Furthermore, for index  $j = 1, \dots, d$ ,  $q_j^{(\boldsymbol{\alpha})}(v_{\alpha_1}, \dots, v_{\alpha_j}) = q_j(\tilde{v}_1, \dots, \tilde{v}_p)$  and  $q_j(\tilde{v}_1, \dots, \tilde{v}_p) = \phi_{L+1}(\widehat{W}_{L+1j} \cdot \mathbf{a}_L + \hat{\mathbf{b}}_{L+1})$ , where  $\mathbf{a}_l = \phi_l(\widehat{W}_l \mathbf{a}_{l-1} + \hat{\mathbf{b}}_l)$  for  $l = 1, \dots, L$  with  $\mathbf{a}_0 = F_{\mathbf{Z}}^{-1}(\tilde{\mathbf{v}})$  and where  $\widehat{W}_{L+1j}$  denotes the  $j$ th row of  $W_{L+1}$ .

Based on the decomposition in (12), a sufficient condition to ensure that  $V(h) < \infty$  is that all products of the form

$$\frac{\partial^{|\boldsymbol{\beta}|_1} \Psi}{\partial^{\beta_1} y_1 \dots \partial^{\beta_d} y_d} \prod_{m=1}^i \frac{\partial^{|\boldsymbol{\kappa}_m|_1} q_{k_m}^{(\boldsymbol{\alpha})}(v_{\alpha_1}, \dots, v_{\alpha_j})}{\partial^{\kappa_{mj}} v_{\alpha_j} \dots \partial^{\kappa_{m1}} v_{\alpha_1}}, \quad i = 1, \dots, j,$$

are integrable.

To that end, Assumptions 2)–4) imply that all mixed partial derivatives of  $q = f_{\hat{\theta}} \circ F_{\mathbf{Z}}^{-1}$  are bounded. By the assumption of continuous partial derivatives of  $q$ , this implies that finite products of the form

$$\prod_{m=1}^i \frac{\partial^{|\boldsymbol{\kappa}_m|_1} q_{k_m}^{(\boldsymbol{\alpha})}(v_{\alpha_1}, \dots, v_{\alpha_j})}{\partial^{\kappa_{mj}} v_{\alpha_j} \dots \partial^{\kappa_{m1}} v_{\alpha_1}}, \quad i = 1, \dots, j,$$

are integrable. By Assumption 1), Decomposition (12) and Hölder's inequality, the quantity in (11) is bounded. This implies that  $h$  has bounded variation, so that the Koksma–Hlawka bound is finite.  $\square$

The following remark provides insights into Assumptions 2)–4) of Proposition A.1.

### Remark A.2

$U(a, b)^p$  for  $a < b$ , which is a popular choice for the prior distribution, clearly satisfies Assumption 2) in Proposition A.1. Assumption 3) is satisfied for various commonly used activation functions, such as:

- 1) *Sigmoid*. If  $\phi_l(x) = 1/(1 + e^{-x})$  for layer  $l$ , then  $N_l = 1$ .

- 2) *ReLU*. If  $\phi_l(x) = \max\{0, x\}$  for layer  $l$ , then  $N_l = 1$ . In this case, only the first derivative is (partly) non-zero. Additionally, note that the ReLU activation function is not differentiable at  $x = 0$ . However, even if  $\phi_l = \max\{0, x\}$  for all  $l = 1, \dots, L + 1$ , the set of all pointwise discontinuities of the mixed partial derivatives of  $q$  is a null set. Hence, the discontinuities do not jeopardize the proof of Proposition A.1.
- 3) *Softplus*. If  $\phi_l(x) = \log(1 + e^x)$  for layer  $l$ , then  $N_l = 1$ . The Softplus activation function can be used as a smooth approximation of the ReLU activation function.
- 4) *Linear*. If  $\phi_l(x) = x$  for layer  $l$ , then  $N_l = 1$ . Only the first derivative is non-zero.
- 5) *Tanh*. If  $\phi_l(x) = \tanh(x)$  for layer  $l$ , then  $N_l = 1$ .
- 6) *Scaled exponential linear unit (SELU)*; see Klambauer et al. (2017). If, for layer  $l$ ,

$$\phi_l(x) = \begin{cases} \lambda\alpha(\exp(-x) - 1), & \text{if } x < 0, \\ \lambda x, & \text{if } x \geq 0, \end{cases}$$

where  $\lambda$  and  $\alpha$  are prespecified constants, then  $N_l = \max\{\lambda, \lambda\alpha, 1\}$ . The same argument about discontinuities made with the ReLU activation function applies equally well to the case of the SELU activation function.

Assumption 4) of Proposition A.1 is satisfied in practice because NNs are always trained with regularization on the parameters, which means  $\hat{\theta}$  always lies in a compact set. Additionally note that in the general case where  $q$  is characterized by a composition of NN layers and  $F_Z^{-1}$  with a different (but standard) activation function in each layer, all partial derivatives of  $q$  exist and are continuous. Moreover, for the activation functions and prior distributions listed above, all mixed partial derivatives of  $q$  are bounded.

### A.3 RQMC point sets

In Monte Carlo applications, we need to randomize the low-discrepancy sequence  $P_{n_{\text{gen}}}$  to obtain unbiased estimators and variance estimates. To that end, we can randomize  $P_{n_{\text{gen}}}$  via a  $\mathbf{U}' \sim \text{U}(0, 1)^p$  to obtain a randomized point set  $\tilde{P}_{n_{\text{gen}}} = \tilde{P}_{n_{\text{gen}}}(\mathbf{U}') = \{\tilde{\mathbf{v}}_1, \dots, \tilde{\mathbf{v}}_{n_{\text{gen}}}\}$ , where  $\tilde{\mathbf{v}}_i = r(\mathbf{U}', \mathbf{v}_i)$ ,  $i = 1, \dots, n_{\text{gen}}$ , for a certain randomization function  $r$ . A simple randomization to obtain an RQMC point set is to consider  $\tilde{\mathbf{v}}_i = (\mathbf{v}_i + \mathbf{U}') \bmod 1$ ,  $i = 1, \dots, n_{\text{gen}}$ , for  $\mathbf{U}' \sim \text{U}(0, 1)^p$ , a so-called *random shift*; see Cranley and Patterson (1976).

In practice, more sophisticated alternatives to the random shift are often used. One such slightly more sophisticated randomization scheme is the *digital shift* method; see Lemieux (2009, Chapter 6) and Cambou et al. (2017). In the same vein as the random shift, one adds a random uniform shift to points in  $P_{n_{\text{gen}}}$ , but with operations in  $\mathbb{Z}_b$ , where  $b$  is the base in which the digital net is defined, rather than simply adding two real numbers. We use  $\tilde{P}_{n_{\text{gen}}}^{\text{ds}}$  to denote the RQMC point set obtained using the digital shift method.

Another randomization approach is to *scramble* the digital net. This technique was originally proposed by Owen (1995). In particular, the type of scrambling we work with is referred to as the *nested uniform scrambling* (or *full random scrambling*) method; see

Owen (2003). Since we primarily use this method throughout the paper,  $\tilde{P}_{n_{\text{gen}}}$  will denote specifically the RQMC point set obtained using scrambling. The digital shift method is more computationally efficient in comparison to scrambling but because the distortion of the deterministic point set is fairly simple in the digital shift method, there are *bad* functions one can construct such that the variance of the RQMC estimator is larger than that of the corresponding MC estimator; see Lemieux (2009, Chapter 6). Furthermore, when RQMC points are constructed with scrambling, we can justify (see Appendix A.4) that an improved rate of  $O(n_{\text{gen}}^{-3}(\log n_{\text{gen}})^{p-1})$  is achievable for  $V(\mu_{n_{\text{gen}}})$ ; this translates to  $O(n_{\text{gen}}^{-3/2}(\log n_{\text{gen}})^{(p-1)/2})$  on the root mean squared error (RMSE) scale, which is more directly comparable to the convergence rate of  $O(n_{\text{gen}}^{-1}(\log n_{\text{gen}})^p)$  implied by the Koksma-Hlawka bound for the mean absolute error (MAE) of  $\mu_{n_{\text{gen}}}$  using QMC points (see Appendix A.2). Hence, even though the aforementioned bad functions do not often arise in practice, we primarily work with the scrambling randomization method to construct our RQMC point sets. Both the digital shift and the scrambling methods are available in the R package `qrng` and can be accessed via `sobol(, randomize = "Owen")` and `sobol(, randomize = "digital.shift")` respectively.

The randomization schemes discussed above preserve the low-discrepancy property of  $P_{n_{\text{gen}}}$  and the estimators of interest obtained using each type of RQMC point set are unbiased. Computing the estimator based on  $B$  such randomized point sets and computing the sample variance of the resulting  $B$  estimates then allows us to estimate the variance of the estimator of interest.

## A.4 Analyzing the GMMN RQMC estimator

### A.4.1 GMMN RQMC estimators constructed with scrambled nets

For RQMC estimators  $\frac{1}{n_{\text{gen}}} \sum_{i=1}^{n_{\text{gen}}} g(\mathbf{v}_i)$  based on scrambled nets, Owen (1997) initially derived a convergence rate for the variance of the estimators under a certain smoothness condition on  $g$ , where  $g : [0, 1]^p \rightarrow \mathbb{R}$ . Owen (2008) then generalized his earlier result to allow a weaker smoothness condition for a larger class of scrambled nets. Specifically, if  $\tilde{P}_{n_{\text{gen}}} = \{\tilde{\mathbf{v}}_1, \dots, \tilde{\mathbf{v}}_{n_{\text{gen}}}\}$  is a so-called relaxed scrambled  $(\lambda, q, m, p)$ -net in base  $b$  with bounded gain coefficients – for example, Sobol' sequences randomized using nested uniform sampling belong to this class – then we have the following result as a direct consequence of Owen (2008).

#### Theorem A.3 (Owen (2008))

If all the mixed partial derivatives (up to order  $p$ ) of  $g$  exist and are continuous, then

$$V\left(\frac{1}{n_{\text{gen}}} \sum_{i=1}^{n_{\text{gen}}} g(\mathbf{v}_i)\right) = O(n_{\text{gen}}^{-3}(\log n_{\text{gen}})^{p-1}).$$

*Proof.* See Owen (2008, Theorem 3). □

## A Analyzing GMMN QMC and GMMN RQMC estimators

Now, for the GMMN RQMC estimator,  $\mu_{n_{\text{gen}}} = \frac{1}{n_{\text{gen}}} \sum_{i=1}^{n_{\text{gen}}} \Psi(q(\tilde{\mathbf{v}}_i)) = \frac{1}{n_{\text{gen}}} \sum_{i=1}^{n_{\text{gen}}} h(\tilde{\mathbf{v}}_i)$ , the corollary below naturally follows from Theorem A.3 with some added analysis of the composite function  $h$ .

### Corollary A.4

If all the mixed partial derivatives (up to order  $p$ ) of  $h = \Psi \circ q = \Psi \circ f_{\hat{\theta}} \circ F_{\mathbf{Z}}^{-1}$  exist and are continuous, then  $V(\mu_{n_{\text{gen}}}) = O(n_{\text{gen}}^{-3} (\log n_{\text{gen}})^{p-1})$ .

To analyze the mixed partial derivatives of  $h$ , it suffices to analyze each component function separately.

For popular choices of prior distributions (such as  $U(a, b)^p$  for  $a < b$  or  $N(0, 1)^p$ ), the  $k$ -fold derivative  $D^k F_{Z_j}^{-1}$  exists and is continuous (on  $[a, b]$  or  $\mathbb{R}$  depending on the choice of prior) for each  $k, j = 1, \dots, p$ .

For each layer  $l = 1, \dots, L+1$  of the NN  $f_{\hat{\theta}}$ ,  $D^k \phi_l$  exists and is continuous for  $k = 1, \dots, p$  – provided that we use (standard) activation functions; see Remark A.2 for further details on suitable activation functions. For NNs constructed using some popular activation functions such as the ReLU and SELU, note that the set of all pointwise discontinuities of the mixed partial derivatives of  $f_{\hat{\theta}}$  is a set of Lebesgue measure zero and hence the proof of Theorem A.3 holds. Alternatively, we can use the softplus activation function as a smoother approximation of ReLU. Now in the most general case of NNs  $f_{\hat{\theta}}$  being composed of layers with different (but standard) activation functions, all mixed partial derivatives (up to order  $p$ ) of  $f_{\hat{\theta}}$  exist and are continuous.

Finally, it is certainly true that, for many functionals  $\Psi$  that we care about in practice, e.g.,  $\Psi_1, \Psi_2, \Psi_3$  and  $\Psi_4$  considered in Section 4, all of its mixed partial derivatives (up to order  $p$ ) exist and are continuous on  $\mathbb{R}^d$ .

### A.4.2 GMMN RQMC estimators constructed with digitally shifted nets

For GMMN RQMC estimators  $\mu_{n_{\text{gen}}}^{\text{ds}}$  constructed using digitally shifted RQMC point sets  $\tilde{P}_{n_{\text{gen}}}^{\text{ds}}$ , we can obtain an expression for  $V(\mu_{n_{\text{gen}}}^{\text{ds}})$  under the condition that the composite function  $h$  is square integrable; see Cambou et al. (2017, Proposition 6).

With added assumptions on the smoothness of  $h$ , one can obtain improved convergence rates (compared to MC estimators) for  $V(\mu_{n_{\text{gen}}}^{\text{ds}})$ . For example, under the assumptions of Proposition A.1,  $h$  has finite bounded variation in the sense of Hardy–Krause, which implies that  $V(\mu_{n_{\text{gen}}}^{\text{ds}}) = O(n_{\text{gen}}^{-2} (\log n_{\text{gen}})^{2p})$ ; see L’Ecuyer (2016).

In practice, we observe that GMMN RQMC estimators constructed using both scrambled and digitally shifted nets achieve very similar convergence rates despite differences in the theoretical convergence rates. To that end, Figure 14 shows plots of standard deviation estimates for estimating  $E(\Psi_4(\mathbf{X}))$  where we use the RQMC point sets  $\tilde{P}_{n_{\text{gen}}}^{\text{ds}}$  for the same copula models as considered for Figure 13 (which is based on GMMN RQMC estimators constructed using scramble nets) in Section 4. The approximate convergence rates as implied by the regression coefficients  $\alpha$  displayed in both figures are very similar across the various examples.

## A Analyzing GMMN QMC and GMMN RQMC estimators

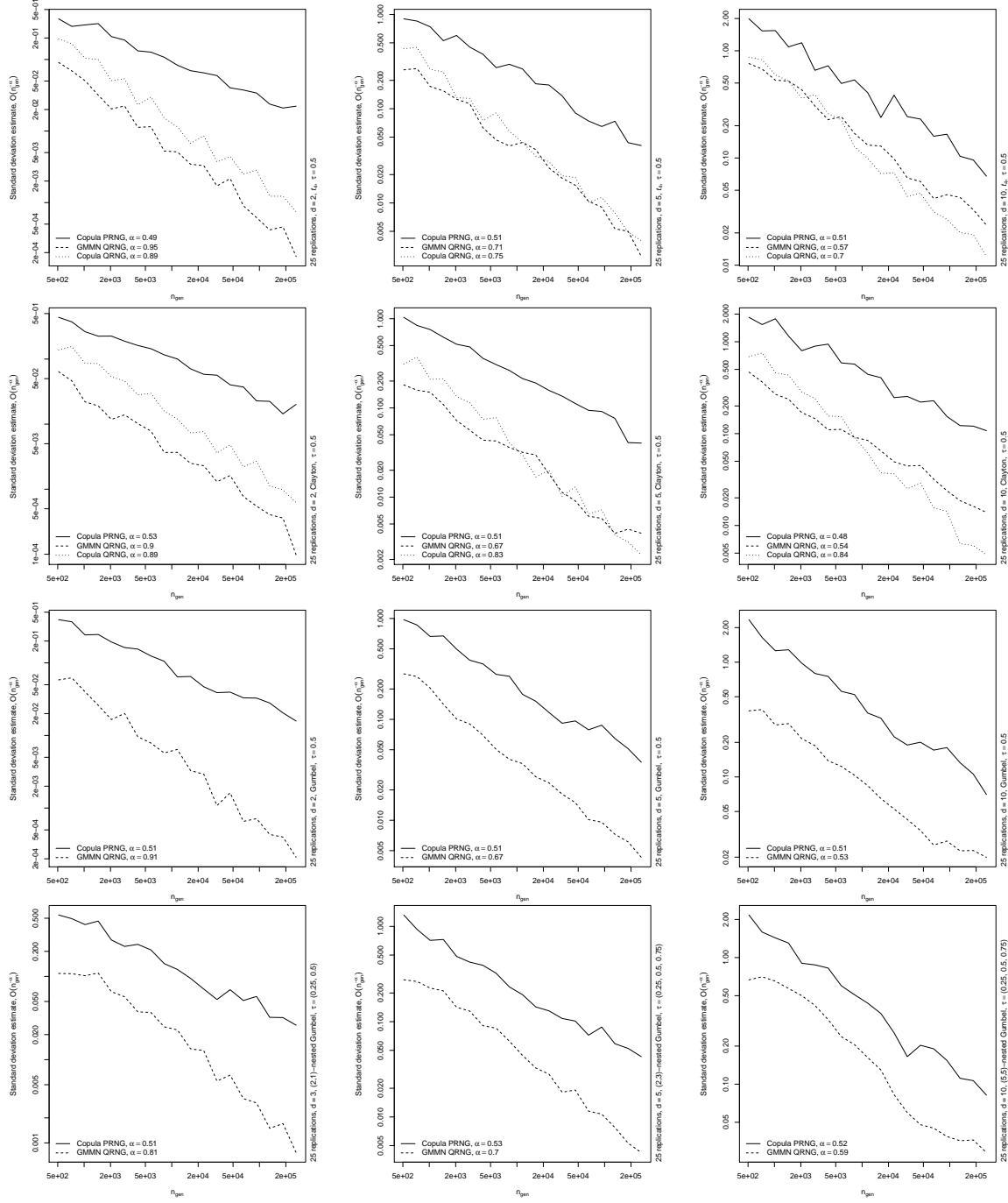


**Figure 14** Standard deviation estimates based on  $B = 25$  replications for estimating  $\mathbb{E}(\Psi_4(\mathbf{X}))$  via MC based on a PRNG, via the copula RQMC estimator (whenever available; rows 1–2 only) and via the GMMN RQMC estimator (based on digitally shifted nets). Note that in rows 1–3,  $d \in \{2, 5, 10\}$ , whereas in row 4,  $d \in \{3, 5, 10\}$ .

## References

Arjovsky, Martin, Chintala, Soumith, and Bottou, Léon (2017), Wasserstein generative adversarial networks, *International conference on machine learning*, 214–223.

Arora, Raman, Basu, Amitabh, Mianjy, Poorya, and Mukherjee, Anirbit (2016), Understanding deep neural networks with rectified linear units, <https://arxiv.org/abs/1611.01491> (11/01/2018).

Arora, Sanjeev, Risteski, Andrej, and Zhang, Yi (2018), Do GANs learn the distribution? Some Theory and Empirics, *International Conference on Learning Representations, ICLR*.

Cambou, Mathieu, Hofert, Marius, and Lemieux, Christiane (2017), Quasi-random numbers for copula models, *Statistics and Computing*, 27(5), 1307–1329.

Constantine, G. and Savits, T. (1996), A multivariate Fa  di Bruno formula with applications, *Transactions of the American Mathematical Society*, 348(2), 503–520.

Cranley, R. and Patterson, T. N. L. (1976), Randomization of Number Theoretic Methods for Multiple Integration, *SIAM Journal on Numerical Analysis*, 13(6), 904–914.

Cybenko, George (1989), Approximation by superpositions of a sigmoidal function, *Mathematics of control, signals and systems*, 2(4), 303–314.

Dziugaite, Gintare Karolina, Roy, Daniel M, and Ghahramani, Zoubin (2015), Training generative neural networks via maximum mean discrepancy optimization, *Proceedings of the Thirty-First Conference on Uncertainty in Artificial Intelligence*, AUAI Press, 258–267, <http://www.auai.org/uai2015/proceedings/papers/230.pdf> (08/24/2019).

E. Hlawka (1961),  ber die Diskrepanz mehrdimensionaler Folgen mod 1, *Mathematische Zeitschrift*, 77, 273–284.

Genest, Christian, R millard, Bruno, and Beaudoin, David (2009), Goodness-of-fit tests for copulas: A review and a power study, *Insurance: Mathematics and economics*, 44(2), 199–213.

Glorot, Xavier and Bengio, Yoshua (2010), Understanding the difficulty of training deep feedforward neural networks, *Proceedings of the thirteenth international conference on artificial intelligence and statistics*, 249–256.

Goodfellow, Ian, Bengio, Yoshua, and Courville, Aaron (2016), Deep learning, vol. 1, MIT press Cambridge.

Gretton, A., Borgwardt, K., Rasch, M. J., Sch lkopf, B., and Smola, A. J. (2007), A kernel method for the two-sample-problem, *Advances in neural information processing systems*, 513–520.

Gretton, A., Borgwardt, K., Rasch, M. J., Sch lkopf, B., and Smola, A. J. (2012), A kernel two-sample test, *Journal of Machine Learning Research*, 13(Mar), 723–773.

Hlawka, E. and M ck, R. (1972),  ber eine Transformation von gleichverteilten Folgen II, *Computing*, 9(2), 127–138.

Hofert, M., Kojadinovic, I., M chl, M., and Yan, J. (2018), Elements of Copula Modeling with R, Springer Use R! Series, ISBN 978-3-319-89635-9, doi:10.1007/978-3-319-89635-9, <http://www.springer.com/de/book/9783319896342> (03/15/2018).

## References

Hofert, Marius (2012), A stochastic representation and sampling algorithm for nested Archimedean copulas, *Journal of Statistical Computation and Simulation*, 82(9), 1239–1255, doi:10.1080/00949655.2011.574632.

Hornik, Kurt (1991), Approximation capabilities of multilayer feedforward networks, *Neural networks*, 4(2), 251–257.

Joe, Harry (2014), Dependence modeling with copulas, Chapman and Hall/CRC.

Kingma, Diederik P and Ba, Jimmy (2014), Adam: A method for stochastic optimization, <https://arxiv.org/abs/1412.6980> (11/01/2018).

Klambauer, Günter, Unterthiner, Thomas, Mayr, Andreas, and Hochreiter, Sepp (2017), Self-normalizing neural networks, *Advances in Neural Information Processing Systems*, 971–980.

L'Ecuyer, Pierre (2016), Randomized quasi-Monte Carlo: An introduction for practitioners, *International Conference on Monte Carlo and Quasi-Monte Carlo Methods in Scientific Computing*, Springer, 29–52.

Lemieux, Christiane (2009), Monte Carlo and Quasi-Monte Carlo Sampling, Springer.

Li, Yujia, Swersky, Kevin, and Zemel, Rich (2015), Generative moment matching networks, *International Conference on Machine Learning*, 1718–1727.

McNeil, A. J. (2008), Sampling nested Archimedean copulas, *Journal of Statistical Computation and Simulation*, 78(6), 567–581.

McNeil, A. J., Frey, R., and Embrechts, P. (2015), Quantitative Risk Management: Concepts, Techniques, Tools, 2nd ed., Princeton University Press.

Montufar, Guido F, Pascanu, Razvan, Cho, Kyunghyun, and Bengio, Yoshua (2014), On the number of linear regions of deep neural networks, *Advances in neural information processing systems*, 2924–2932.

Nelsen, R. B. (2006), An Introduction to Copulas, Springer-Verlag.

Niederreiter, Harald (1992), Random number generation and quasi-Monte Carlo methods, vol. 63, Siam.

Nielsen, M. A. (2015), Neural Networks and Deep Learning, <http://neuralnetworksanddeeplearning.com>, Determination Press, (09/18/2018).

Owen, Art B (1995), Randomly permuted (t, m, s)-nets and (t, s)-sequences, *Monte Carlo and quasi-Monte Carlo methods in scientific computing*, Springer, 299–317.

Owen, Art B (1997), Monte Carlo variance of scrambled net quadrature, *SIAM Journal on Numerical Analysis*, 34(5), 1884–1910.

Owen, Art B (2003), Variance and discrepancy with alternative scramblings, *ACM Transactions of Modeling and Computer Simulation*, 13(4).

Owen, Art B (2008), Local antithetic sampling with scrambled nets, *The Annals of Statistics*, 36(5), 2319–2343.

Pascanu, Razvan, Mikolov, Tomas, and Bengio, Yoshua (2013), On the difficulty of training recurrent neural networks, *International Conference on Machine Learning*, 1310–1318.

Rosenblatt, Murray (1952), Remarks on a multivariate transformation, *The annals of mathematical statistics*, 23(3), 470–472.

## References

Sobol', Il'ya Meerovich (1967), On the distribution of points in a cube and the approximate evaluation of integrals, *Zhurnal Vychislitel'noi Matematiki i Matematicheskoi Fiziki*, 7(4), 784–802.

Tolstikhin, Ilya O, Gelly, Sylvain, Bousquet, Olivier, Simon-Gabriel, Carl-Johann, and Schölkopf, Bernhard (2017), Adagan: Boosting generative models, *Advances in Neural Information Processing Systems*, 5424–5433.